



Search for a Higgs boson decaying into a b-quark pair and produced in association with b quarks in proton-proton collisions at 7 TeV

The CMS Collaboration*

Abstract

A search for a neutral Higgs boson decaying to a pair of b quarks, and produced in association with at least one additional b quark, is presented. Multijet final states with three jets identified as originating from b quarks, at least one of which may include a non-isolated muon, are studied. The data used in this analysis correspond to an integrated luminosity of $2.7\text{--}4.8\text{ fb}^{-1}$, collected by the CMS experiment in proton-proton collisions at the LHC at a center-of-mass energy of 7 TeV. This search is particularly sensitive to Higgs bosons in scenarios of the Minimal Supersymmetric Model (MSSM) with large values of $\tan\beta$. No excess over the predicted background from standard model processes is observed. Stringent upper limits on cross section times branching fraction are derived and interpreted as bounds in the MSSM $\tan\beta$ and M_A parameter-space. Observed 95% confidence level upper limits reach as low as $\tan\beta \approx 18$ for $M_A \approx 100\text{ GeV}$.

Submitted to Physics Letters B

1 Introduction

The electroweak symmetry breaking mechanism of the standard model (SM) predicts the existence of a neutral scalar boson, the Higgs particle. A boson has been recently discovered, with a mass around 125 GeV [1, 2] and properties consistent with those expected for the SM Higgs boson. However, its exact properties and the detailed structure of the Higgs sector still need further investigation. Moreover, the mass of the Higgs boson is quadratically divergent at high energies [3]. Supersymmetry [4] is a well known extension to the SM which allows the cancellation of this divergence.

In contrast to the SM, the Minimal Supersymmetric Standard Model (MSSM) [5] features two scalar Higgs doublets, giving rise to three neutral Higgs bosons, collectively denoted as ϕ , and two charged ones, H^\pm . Two of the neutral bosons are CP-even (h, H) and one is CP-odd (A). In this context, the recently discovered boson with a mass near 125 GeV might be interpreted as one of the neutral CP-even states. At tree level, two parameters, conventionally chosen as the mass of the pseudoscalar Higgs boson M_A and the ratio of the vacuum expectation values of the two Higgs doublets, $\tan\beta = v_2/v_1$, define the Higgs sector in the MSSM. For $\tan\beta$ larger than unity, the Higgs field couplings to up-type particles are suppressed relative to the SM, while the couplings to down-type particles are enhanced by a factor of $\tan\beta$. In addition, the mass M_A is expected to be nearly degenerate with either M_h or M_H . Therefore, the combined cross section of Higgs boson production in association with b quarks is effectively enhanced by a factor $\approx 2 \tan^2\beta$. Moreover, the decay into b quarks has a very high branching fraction ($\approx 90\%$), even at large values of the Higgs boson mass M_A . The sensitivity for a SM Higgs boson search for the corresponding channel is negligible given the small cross section.

Recent results at the Large Hadron Collider (LHC) on the $\phi \rightarrow \tau\tau$ decay mode [6, 7] provide stringent constraints on $\tan\beta$, complementing previous results from the LEP experiments [8] and superseding those from the Tevatron experiments [9–11]. Similar searches in the $\phi \rightarrow b\bar{b}$ decay mode have also been performed by the CDF and D0 experiments [12] at the Tevatron collider. An excess of events of ≈ 2 standard deviations with respect to the expectations from SM background have been reported by both experiments for a resonance in the mass range 100–150 GeV.

In this Letter we present a search for MSSM neutral Higgs bosons produced in association with at least one b quark, and decaying into a pair of b quarks. Prospects for this channel at the LHC have been studied in Refs. [13, 14]. This analysis is performed using $2.7\text{--}4.8 \text{ fb}^{-1}$ of proton-proton collisions with a center-of-mass energy of 7 TeV collected in 2011 by the Compact Muon Solenoid (CMS) detector at the LHC. The dominant background is the production of heavy-flavor multijet events containing either three b jets, or two b jets plus a third jet originating from either a charm or a light-flavor parton, which is misidentified as a b jet.

A signal is searched for in final states characterized either purely by jets (“all-hadronic”) or with an additional non-isolated muon (“semileptonic”). Events are selected by specialized triggers that include online algorithms for the identification of b jets to tackle the large multijet production rate at the LHC. The common analysis strategy is to search, in events identified as having at least three b jets, for a peak in the invariant mass distribution of the two leading b jets, i.e. those having the largest transverse momentum, over the large multijet background. A key point of both analyses is the estimation of the background using control data samples, which is addressed with different methods. The two analyses reach similar sensitivity to the MSSM Higgs scenarios described. The corresponding data sets are largely exclusive, and the small overlap is removed for the combined results.

2 The CMS experiment

The central feature of the CMS detector is a superconducting solenoid of 6 m internal diameter, providing a magnetic field of 3.8 T. Within the field volume, the inner tracker is formed by a silicon pixel and strip tracker. It measures charged particles within the pseudorapidity range $|\eta| < 2.5$. The pseudorapidity is defined as $\eta = -\ln(\tan(\theta/2))$ and θ is the polar angle, while ϕ is the azimuthal angle in radians. The tracker provides an impact parameter resolution of approximately $15 \mu\text{m}$ and a resolution on transverse momentum (p_T) of about 1.5% for 100 GeV particles. Also inside the field volume are a crystal electromagnetic calorimeter and a brass/scintillator hadron calorimeter. Muons are measured in gas-ionization detectors embedded in the iron flux return yoke, in the pseudorapidity range $|\eta| < 2.4$, with detector planes made using three technologies: drift tubes, cathode-strip chambers, and resistive-plate chambers. Matching muons to tracks measured in the silicon tracker results in a transverse momentum resolution between 1% and 5%, for p_T values up to 1 TeV. Extensive forward calorimetry complements the coverage provided by the barrel and endcap detectors. A more detailed description of the CMS detector can be found in Ref. [15].

3 Event reconstruction and simulation

The CMS particle-flow event reconstruction [16, 17] is used for optimized reconstruction and identification of all particles in the event, i.e. electrons, muons, photons, charged hadrons, and neutral hadrons, with an extensive combination of all CMS detectors systems.

The reconstructed primary vertex with the largest p_T^2 -sum of its associated tracks is selected and used as reference for the other physics objects.

Jets are reconstructed using the anti- k_T algorithm [18] from particle-flow objects with a radius parameter $R = 0.5$ in the rapidity-azimuthal angle space. Each jet is required to have more than one track associated to it, and to have electromagnetic and hadronic energy fractions of at least 1% of the total jet energy. Additional proton-proton interactions within the same bunch crossing (pileup) affect the jet momentum reconstruction. To mitigate this effect, a track-based algorithm that removes all charged hadrons not originating from the primary interaction is used. In addition, a calorimeter-based algorithm evaluates the energy density in the calorimeter from interactions not related to the primary vertex, and subtracts it from the reconstructed jets in the event. Additional jet energy corrections [19] are applied.

Muons are reconstructed using both the inner silicon tracker and the outer muon system [20], and by performing a global track fit seeded by signals in the muon system.

The combined secondary vertex (CSV) algorithm [21] is used in the offline identification of b jets. The CSV algorithm uses information on track impact parameter and secondary vertices in a jet combined in a likelihood discriminant that provides a good separation between b jets and jets of other flavors. Secondary-vertex reconstruction is performed with an inclusive vertex search amongst the tracks associated to a jet [22].

Simulated samples of signal and background events were produced using various event generators and including pileup events. The CMS detector response is modeled with GEANT4 [23]. The MSSM Higgs signal samples, $pp \rightarrow b\bar{b}\phi + X$, $\phi \rightarrow b\bar{b}$, were produced with PYTHIA v6.424 [24], which yields the p_T and η distributions of the leading associated b jet in good agreement with the NLO calculations [25]. The Quantum Chromodynamics (QCD) multijet background events were produced with PYTHIA and ALPGEN [26], while for $t\bar{t} + \text{jets}$ events the MADGRAPH [27] event generator was used. The next-to-leading order generators are interfaced with PYTHIA.

For all generators, fragmentation, hadronization, and the underlying event are modelled using PYTHIA with tune Z2. The parton density functions (PDF) from CTEQ6L1 [28] are used.

4 All-hadronic signature

We search for the Higgs boson in events where the three leading jets are all b-tagged. A signal would be identified as a peak in the invariant mass distribution of the two leading jets. Events in the data with only two b tags among the three leading jets are used to model the background, after proper reweighting, as described in Section 4.2.

4.1 Trigger and event selection

The large hadronic interaction rate at the LHC poses a major challenge for triggering. Events are accepted if either two or three jets are produced in the pseudorapidity range $|\eta| < 2.6$ and have p_T above certain thresholds. Due to the increase in instantaneous luminosity as the run progressed the jet triggers had to be changed. Thus the data is divided into three categories. The first (second) category is characterized by dijet triggers in which the leading jet is required to have $p_T > 46$ (60) GeV, and the next-to-leading jet $p_T > 38$ (53) GeV. The third category is similar to the first but requires a third jet with $p_T > 20$ GeV. The online identification of b jets is performed by an algorithm based on the impact parameter significance of the second most significant track associated to the jet as the b-tagging discriminant. Only events with at least two jets passing the online b-tagging requirement are accepted by the trigger.

The triggers with lower thresholds allow for a better exploration of the low mass region, albeit with smaller integrated luminosity. The inclusion of the higher-threshold triggers allows higher integrated luminosity, but with the adjusted analysis requirements only the medium to high mass region can be covered. For this reason two analysis scenarios are defined: in the low-mass scenario ($M_\phi < 180$ GeV), events accepted by the low jet p_T threshold triggers (first and third categories) are selected corresponding to an integrated luminosity of 2.7 fb^{-1} . In the medium-mass scenario ($180 \leq M_\phi \leq 350$ GeV), a combination of dijet triggers with low and high jet p_T thresholds (first and second categories) forms an event sample with an integrated luminosity corresponding to 4.0 fb^{-1} .

Events are required to have at least three reconstructed jets with $|\eta| < 2.2$, where the b-tag efficiency and mistag probability are essentially constant. The three leading jets must also pass the p_T cuts of 46, 38 and 20 GeV (60, 53 and 20 GeV), respectively, in the low- (medium-) mass scenario. A minimal separation of $\Delta R > 1$ between the two leading jets, where $\Delta R = \sqrt{(\Delta\eta)^2 + (\Delta\phi)^2}$ and $\Delta\eta$ and $\Delta\phi$ are the pseudorapidity and azimuthal angle differences between the two jets, is required to suppress background from gluon splitting to a b-quark pair.

We define a “triple-b-tag” sample to search for a signal by requiring all three leading jets to pass a tight CSV b-tagging selection requirement, consistent with the online b-tagging demand, at a working point characterized by a misidentification probability for light-flavor jets of about 0.1% at an average jet p_T of 80 GeV. The average b-tagging efficiency for true b jets is about 55% for jets with $80 < p_T < 120$ GeV. The total numbers of events passing the trigger and offline selections are 106 626 and 89 637 for the low- and medium-mass scenarios, respectively. The efficiency of the trigger for signal events passing the offline selection is 47–67%, for a Higgs boson mass in the range of 90–350 GeV.

We define a “double-b-tag” sample, which is instrumental in estimating the shape of the background, where only two of the three leading jets have to pass the above-mentioned criteria,

while the remaining untagged jet does not have to fulfill any b-tagging requirements. Since the double-b-tag sample is dominated by QCD events with two b jets, it represents a control region suitable to model the shape of the background contribution.

The secondary-vertex mass, namely the invariant mass calculated from all tracks forming the secondary vertex, provides an additional separation between b-, c- and light-flavor jets (attributed to u, d, s, or g partons) beyond the CSV b-tagging selection requirement. A compact b-tagging variable for the whole event is constructed by assigning to each selected jet j , where j is the rank of the jet in the order of decreasing p_T , an index B_j which can take one of three possible values. For jets with no reconstructed secondary vertex, or where the secondary vertex mass is below 1 GeV, B_j is set to zero. For intermediate values of the vertex mass between 1–2 GeV the index is set to 1, and for vertex mass larger than 2 GeV it is set to 2. The three indices B_1 , B_2 , and B_3 are combined in an event b-tag variable X_{123} , which is defined as follows: $X_{123} = X_{12} + X_3$, where $X_{12} = 0, 1$ or 2 depending on whether $B_1 + B_2 < 2$, $2 \leq B_1 + B_2 < 3$ or $B_1 + B_2 \geq 3$, respectively, and $X_3 = 0$ if $B_3 < 2$, and $X_3 = 3$ otherwise.

By construction, the event b-tag variable X_{123} can have six possible values ranging from 0 to 5. The intention of this mapping is to have each bin populated with sufficient statistics. For event types with a strong triple b-tag signature, the X_{123} distribution typically shows peaks at values of 2 and 5.

4.2 Background model and signal extraction

The dominant background comes from Quantum Chromodynamics (QCD) multijet production with two or more jets containing b hadrons, and can neither be fully reduced by kinematic selection, nor reliably predicted by Monte Carlo (MC) simulation. For this reason, a method based on control data samples, similar to the one used in Ref. [29] is applied. The background model is constructed from templates that are derived from the double-b-tag sample.

We divide the events in the double-b-tag sample into the following categories: bbx, bxb, and xbb, depending on the rank, sorted by p_T , of the untagged jet, which is represented by the lower-case letter x. The ranking in descending p_T of the three jets is incorporated in the nomenclature adopted here, e.g. bbx means a sample of events where the two leading jets are b tagged and the third jet is the untagged jet. The *true* flavor of the untagged jet can be either light (u,d,s flavor quark, or g, denoted collectively by q), charm (c) or bottom (b).

From these three double-b-tag categories, nine background templates are constructed by weighting each untagged jet with the b-tagging probability assuming that its true flavor corresponds to either a light parton (u, d, s, or g, denoted by Q), a charm (C) or a bottom (B) quark. The convention is that the capital letter indicates the *assumed* flavor of the untagged jet. The b-tagging probability for each flavor is determined as a function of jet p_T and η with simulated multijet events. Data/MC scale factors for the b-tagging efficiencies of b, c, and light flavor jets are applied where appropriate [21].

Each background template is a distribution in the two-dimensional space spanned by M_{12} , the dijet mass of the two leading jets, and the event b-tag variable X_{123} .

The following nine background templates are thus created: Qbb; Cbb; Bbb; bQb; bCb; bBb; bbQ; bbC; and bbB. In the bbb background events, two $b\bar{b}$ pairs are present. As pointed out in Ref. [29], the template bbB models mainly bbb events in which the two leading b quarks originate from the same $b\bar{b}$ pair in the event, while Bbb and bBb are important to cover cases where the two leading b quarks originate from different $b\bar{b}$ pairs.

The X_{123} dimension of the templates is modeled in a similar way. Each of the three possible values of the secondary-vertex mass index of the untagged jet is taken into account with a weight according to the probability that a jet will end up in a given bin of the secondary-vertex mass distribution. These probabilities, parametrized as a function of the jet p_T and η , have been determined for each flavor using jets from simulated $t\bar{t}$ events.

Some of the nine templates are similar to each other in shape both for M_{12} and X_{123} . In the cases where one of the two leading jets is untagged, e.g. Qbb , and bQb , the templates are combined, resulting in a merged template $(Qb)b = Qbb + bQb$. By analogy, also $(Cb)b$ and $(Bb)b$ are obtained. When the third-leading jet is the untagged one and the assumptions of its flavor are either Q or C , the bbQ and the bbC templates are combined to form the template bbX . The total number of templates to be fitted to the data is therefore reduced from nine to five, namely $(Bb)b$, $(Cb)b$, $(Qb)b$, bbB and bbX . The projections of the M_{12} and X_{123} variables are shown in Fig. 1 for the five background templates and for the low-mass scenario.

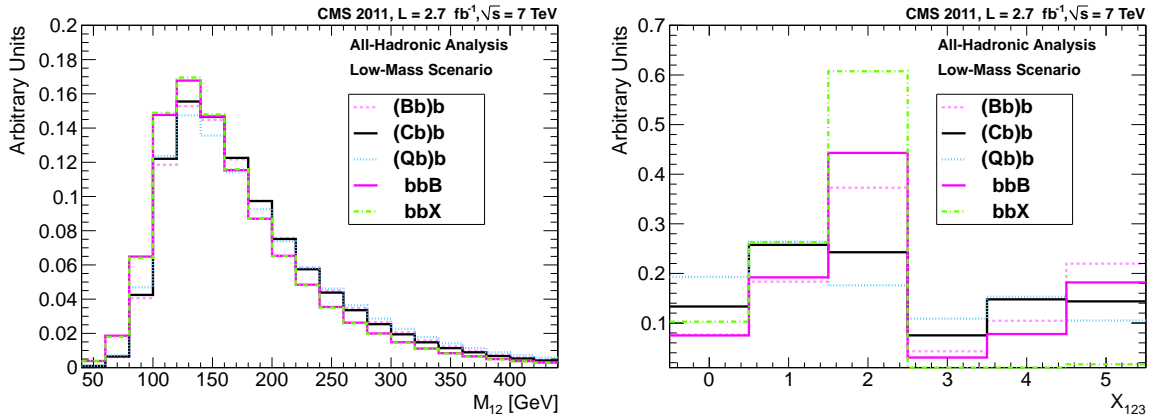


Figure 1: The M_{12} (left) and X_{123} (right) projections of the five background templates, $(Bb)b$, $(Cb)b$, $(Qb)b$, bbB , and bbX , for the low-mass scenario.

Templates whose dijet mass spectra resemble each other can be clearly distinguished with the introduction of the event b-tag variable X_{123} . This is the case for example between $(Bb)b$ and $(Cb)b$. In general, the event b-tag significantly improves the discrimination among all flavor components modeled.

The background templates whose projections are shown in Fig. 1 include two additional corrections. The basic assumption of the background model, that the double-b-tag sample (bb) consists entirely of events with at least two genuine b jets, is only approximately correct. Although the remaining contamination from non- bb events is indeed very small, the impact of the b-tagging selection could lead to distortions of the background model and a correction must be applied. This contamination is estimated directly from the data using a negative b-tagging discriminator [30] constructed with a track-counting algorithm based on the negative impact parameter of the tracks, ordered from the most negative impact parameter significance upward. The set of events in the double-b-tag sample in which at least one of the b-tagged jets passes a certain threshold of the negative b-tagging discriminator is used as a model for the contamination by non- bb events. The threshold is calibrated as a function of jet p_T with simulated multijet events, such that the negative tag rate equals the mistag rate. With this method, the non- bb contribution is found to be at the level of 3–4%. This correction results in only a marginal change in template shape. A second correction is necessary because the online b-tagging patterns differ in the double- and the triple-b-tag samples. The correction is determined from simulation, and is applied by appropriate weighting of the events in the double-b-tag sample.

A signal template is obtained for each considered value of the Higgs boson mass by performing the full selection on the events of the corresponding simulated signal sample. The mass resolution for combinations where both b jets stem from the Higgs decay ranges from 12–14% over the mass range of 90–350 GeV. In addition, combinations with at least one of the b-tagged jets originating from other sources contribute to the signal mass spectrum. The fraction of true combinations within 1σ of the mass resolution increases from 50–90%. Similar figures apply also for the semileptonic signature discussed in Section 5.

The signal is extracted by fitting a linear combination of signal and background templates, $N_{\text{bbb}} (f_{\text{sig}} T_{\text{sig}} + \sum_i f_{\text{bgd}}^{(i)} T_{\text{bgd}}^{(i)})$, to the observed histogram in M_{12} and X_{123} space, where N_{bbb} is the total number of selected triple-b-tag events, $T_{\text{bgd}}^{(i)}$ and T_{sig} are the above-mentioned background and signal templates, each normalized to unity, and $f_{\text{bgd}}^{(i)}$ and f_{sig} are the background and signal fractions determined by the fit. The results of the fit are discussed in Section 7.

5 Semileptonic signature

In the semileptonic signature, as for the all-hadronic one, a signal is searched for in events with three identified b jets, as a peak in the invariant mass distribution of the two leading jets. The expected background distribution and normalization is built using the same distribution for events with three jets of which only one or two are tagged as b jets, reweighting the events with a probability derived from a control region and computed with two different techniques. The muon requirement in the final state reduces the absolute signal efficiency, since it selects events where at least one of the b quarks decayed semileptonically in the muon channel, but it helps to reduce the event rate at the trigger level, allowing for a lower threshold for the jets.

5.1 Trigger and event selection

The data used in the semileptonic analysis were collected using different trigger selections, to cope with the increasing luminosity. All the triggers required a muon with a $p_T > 12$ GeV threshold and the presence of one or two central jets ($|\eta| < 2.6$) with transverse momentum above a given threshold (20 or 30 GeV, depending on the data-taking period). Furthermore, one or two b-tagged jets are required online. Initially the track with the second-most significant impact parameter was used. Later, when a second online b-tag was introduced, the selection was on the first track, in order to retain enough signal efficiency even with this tighter selection. An integrated luminosity of 4.8 fb^{-1} has been analyzed, and about 1.67×10^7 events were collected.

The offline analysis requires a muon with $p_T > 15$ GeV, at least three jets with $|\eta| < 2.6$, having transverse momentum $p_T > 30$ GeV for the first two and $p_T > 20$ GeV for the third one. The separation between any pair of jets has to be $\Delta R > 1$. The two leading jets must be b-tagged using the CSV b-tagging algorithm with a working point giving mistag probability for light jets of about 0.3%. The muon must be contained in one of the two leading jets. The final selection for the signal search adds the requirement that the third jet is also b-tagged, with a looser CSV b-tagging selection requirement, corresponding to a mistag probability of about 1%. The total number of events which pass the selection is 60 195.

The relative efficiencies of the triggers with respect to the offline selection criteria were measured using lower-threshold single-muon triggers. These efficiencies are found to be about 45–60%, depending on the Higgs boson mass and the trigger.

5.2 Background determination and signal extraction

As in the all-hadronic final state, the major backgrounds for the semileptonic final state are multijet events from hard-scattering processes. Other background processes, such as $t\bar{t} + \text{jets}$ and $Z \rightarrow b\bar{b} + \text{jets}$, are predicted by the MC simulation to be less than 1% of the total background. Other possible backgrounds from events with multiple vector bosons (ZZ, ZW, WW) are negligible.

Two methods, both derived from data, have been developed to predict the expected background. The first is based on the computation of b-tagging probabilities of the third jet; and the second is based on a nearest-neighbor-in-parameter-space technique. They are able to predict the yield and shape of the multijet background as well as other minor contributions. The two methods use completely exclusive data samples, so their two predictions are independent. The first method uses double-b-tag samples (bbj) and the second uses single-b-tag samples (bjj) with the double-b-tag events removed.

Both methods require a background-rich sample to serve as a control region. We construct a discriminating variable with a likelihood ratio, using various kinematic inputs: the p_T of the b jets; separation in ϕ and η of the b jets; separation in ϕ and η between the third jet and the combination of the two leading jets; and the b jet multiplicity. Two versions of this discriminating variable are used: one for the low-mass region ($M_\phi \leq 180 \text{ GeV}$) and another for the medium-mass region ($M_\phi > 180 \text{ GeV}$). For both mass ranges, the control region is defined as the sample of events having a low value for the discriminating variable, where the background is enriched and the signal depleted, and the signal region is defined as the complementary sample. The number of events in the signal region is 33 366 and 16 866, for the low- and medium-mass regions, respectively.

The first method, henceforth called the matrix method, uses the probability that a jet is identified as a b jet to predict the background in the signal region. The predicted distribution of any observable x in the three-b-jet sample can be calculated by rescaling, on an event-by-event basis, the same distribution for the bbj sample by the probability P_b of the third jet to be b-tagged. Taking into account the contribution of b, c, and light jets, the probability expands as: $P_b = \epsilon_b \cdot f_b + \epsilon_c \cdot f_c + \epsilon_q \cdot (1 - f_b - f_c)$, where $\epsilon_{b,c,q}$ are the probabilities (or b-tagging efficiencies) for a jet to be b-tagged, if it is originated from b, c, or light parton, respectively. The $f_{b,c}$ are the probabilities that the third jet originates from the corresponding quark, which depend on the kinematics of the event and of the third b jet.

The b-tagging efficiencies are taken from the MC simulation and checked with several methods derived from data [31]. Data/MC scale factors (close to unity within a few percent) are applied for the efficiencies and the corresponding uncertainties used as systematics uncertainties. The efficiencies are parametrized as functions of the third jet p_T, η and charged-particle multiplicities. The quark flavor fractions are obtained directly from data by a simultaneous fit of two flavor-sensitive observables, using templates built from simulated events with b, c and light quarks. The first variable used is a b-tag discriminator which uses the confidence level that the four tracks with the highest impact parameter in the jet are consistent with originating from the primary vertex. The second is the invariant mass associated with the secondary vertex, if it has been reconstructed. The parametrization for quark fractions also depends on the angular separation between the three b jets. Only events in the control region are used to obtain the quark fraction, which is then used to predict the background in both control and signal region.

The second method, called the nearest-neighbor method, exploits the fact that the probability for an event to appear signal-like depends on several event and jet variables. Events from the

background enhanced control region are categorized according to several such variables, and are used to create a multi-parameter background prediction. The method uses the bjj sample, and determines, for each event, the probability to pass the final selection. Starting from the bjj sample, excluding the bjb events, we can identify four disjoint subsets with which we work: (1) bjj (including bjb) in the control region, (2) bbb in the control region, (3) bjj in the signal region, and (4) bbb in the signal region. The sum of the above sets corresponds to the initial sample, where the leading jet is always b-tagged. We call collectively “training sample” the sum of subsets (1) and (2), and “testing sample” the sum of (3) and (4). The probability that an event in the testing sample passes the full selection is estimated by considering a larger sample of “similar” events in the training sample, and counting how many of these events pass the full selection.

For each event in the testing sample, referred to as test events, we select a sample of events with similar kinematics in the training sample. The probability for a test event to pass the final selection is calculated by selecting a sample of 100 training events inside a hyper-ellipsoid in the multi-dimensional space of event and jet observables, centered at the test event. The training events are chosen as those having the smallest multi-dimensional distance D , where $D^2 = \sum_{i=1}^{n_V} w_i^2 (x_i^{\text{test}} - x_i^{\text{training}})^2$, x_i is the variable defining the test and training event, and n_V is the number of variables. The weights w_i account for the different dispersions of the variables and their different sensitivity to the b-tagging probability. A total of $n_V = 14$ different variables are used, including p_T , η and the charged-particle multiplicity of the jets, the angular separation between the jets, and the invariant mass and transverse momentum of the combined jet-jet system. The weights w_i are computed from the derivative of the probability for an event to pass the final selection as a function of the variable x_i . We then compute the numbers of bbb and bjj events inside this training sample. Finally, the probability for test events to have three b-tagged jets is computed as the ratio of bbb to bjj events in the training sample, using a weighted average, with $1/D^2$ as weight. The probability obtained this way is then applied, event-by-event, to the sample of test events to predict the invariant mass distribution of the sample passing the final selection. This method gives a prediction of the background shape in the signal region independent from that obtained with the matrix method.

The background predictions for the invariant mass distribution of the two leading jets from the two methods described above are shown in Fig. 2. They are compared with the actual distribution in events with three b-tagged jets in the control region (low value of the discriminator), for low- and medium-mass regions. The predictions are normalized to the number of events seen; the absolute normalization of the prediction will be discussed in Section 6.

Because the matrix and nearest-neighbor methods use exclusive data samples, we can combine their results. This is done by performing a weighted average of their bin-by-bin predictions, using the statistical uncertainties σ_i as weights ($w = 1/\sigma_i^2$). In case the χ^2 of the average is greater than 1, $(\sqrt{\chi^2} - 1) \cdot \sigma_i$ is used, bin-by-bin, as an additional systematic uncertainty, following the Particle Data Group prescription [32].

6 Systematic uncertainties

Various systematic uncertainties on the expected signal and background estimates affect the cross section estimation and, consequently, its interpretation within the MSSM. In both analyses the main source of systematic uncertainty on the estimated signal yield comes from uncertainties related to jet reconstruction and b tagging. The second source is the turn-on behavior of the trigger efficiency, given the rather low thresholds used in the event selection. Other sources

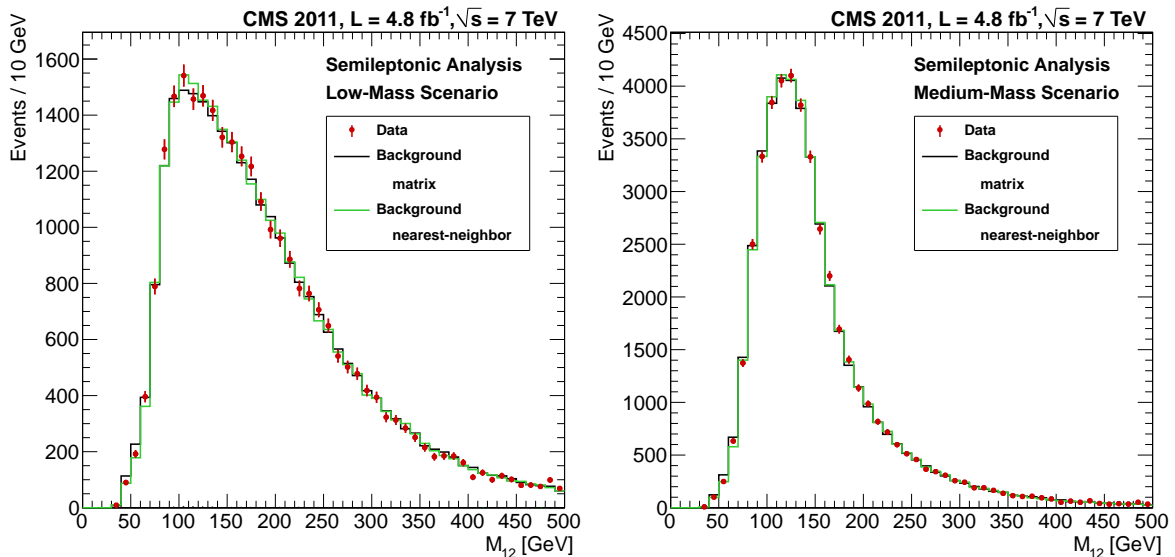


Figure 2: Invariant mass of the two leading jets for data in the control regions, for low- (left) and medium-mass (right) regions. Predictions with matrix (black histogram), with nearest-neighbor methods (green histogram), and data (red dots) are overlaid. The predictions are normalized to the data.

include uncertainties on the integrated luminosity and lepton identification. The theoretical cross sections used for the MSSM interpretation are subject to factorization and renormalization scale uncertainties, uncertainties due to the choice of parton distribution functions and α_s , and uncertainties from the underlying event and parton shower modelling [33]. These uncertainties affect only the computation of the upper limits for the MSSM parameter $\tan\beta$ from the cross section results. The systematic effects directly affecting the signal efficiency, hence the cross section and MSSM interpretation, are summarized in Table 1.

There are systematic uncertainties that affect only the all-hadronic or semileptonic analyses. In the all-hadronic analysis, Table 1 includes systematic uncertainties related to the efficiency of the online b-tag selection relative to that applied offline, and to a slight dependence of the b-tagging efficiency on the jet topology. Various uncertainties also affect the shapes of the signal and background templates used in the fit. Shape-altering effects from uncertainties on the jet energy scale, jet energy resolution, b-tagging efficiency and mistag rates are accounted for in the fits with nuisance parameters. For the background templates, only the latter two are relevant. In the following we quantify background-related systematic uncertainties by their effect on the estimated signal fraction f_{sig} (defined in Section 4). The uncertainty arising from the jet energy scale and the b-tagging efficiency on the template shape increases the f_{sig} uncertainty by typically 0.1–0.4%; the corresponding effect from the jet energy resolution uncertainty is 0.1–0.3%. Additional shape-altering systematic uncertainties arise from the impurity of the double-b-tag sample and the online b-tagging correction to the background templates shape. The contribution of the former to the f_{sig} systematic uncertainty ranges between 0.1–0.3% in the mass range 90–130 GeV, and is below 0.1% elsewhere. The effect of the latter correction ranges from 0.1% to 0.4% in the mass range 90–160 GeV, and is below 0.1% elsewhere. The statistical uncertainty on the offline b-tagging efficiency values is propagated into the templates and accounted for in the fitting procedure. The impact on the f_{sig} uncertainty is typically in the range 0.1–0.6%.

In the semileptonic analysis there are uncertainties on both the background shape and normalization. The shape-related uncertainty is inferred by the comparison of the background

Table 1: Systematic uncertainties on the signal yield from the various sources listed in the first column. The following two columns list the resulting uncertainties in the all-hadronic and semileptonic analyses. The upper group is for the signal, the lower for the model-dependent limits. A range indicates the variation across the probed Higgs boson mass values. The source with [†] also affects the background, while those with * only affect the model-dependent results in the space of the MSSM parameters M_A and $\tan\beta$. The sources labeled with “rate” affect only the total signal yield, those with “shape” also the shape of the signal.

Source	All-hadronic	Semileptonic	Type
Trigger efficiency	10%	3 – 5%	rate
Online b-tagging efficiency	32%	–	rate
Offline b-tagging efficiency	10–13% [†]	12%	shape/rate
b-tagging efficiency dependence on topology	6%	–	rate
Jet energy scale	1.4–6.8%	3.1%	shape/rate
Jet energy resolution	0.6–1.3%	1.9%	shape/rate
Muon momentum scale and resolution	–	1%	rate
Signal Monte Carlo statistics	1.1–2.6%		rate
Integrated luminosity	2.2%		rate
PDF and α_s uncertainties	3–6%*	2.7–4.7%*	rate
Factorization and renormalization QCD scale	6–28%*		rate
Underlying event and parton showering	4%*		rate

predictions obtained with the two methods described in Section 5.2. The corresponding uncertainty scaling is included on a bin-by-bin basis in the binned maximum likelihood fit to the distribution of the final observable. The background normalization uncertainty has two components: the first is related to the level of agreement between the predicted M_{12} distribution and the actual bbb one in the data control region and the second is related to the extrapolation of this prediction from the control region to the signal region. The ratio between the predicted M_{12} distribution and the actual bbb one in the control region as seen in the data is used to normalize the prediction in the signal region, and its uncertainty is used as a systematic uncertainty. The scale factor is 0.877 ± 0.007 for the low-mass region and 0.885 ± 0.006 for the medium-mass region. For the extrapolation from the control region to the signal region, the MC simulation shows a constant ratio between the predicted M_{12} distribution and the actual bbb one in the signal region. The additional correction is 1.01 ± 0.04 and 1.02 ± 0.05 for the low- and medium-mass regions, respectively. The uncertainties on these corrections are used as systematic uncertainties for the background normalization: 4.4% and 5.0% for the low- and medium-mass ranges, respectively.

7 Results

In the all-hadronic analysis, we first test the background-only hypothesis by performing a χ^2 fit without including a signal template, but only a linear combination of the background templates, as described in Section 4.2. The coefficients $f_{\text{bgd}}^{(i)}$ are free parameters, but are constrained to be positive. Results are shown in Fig. 3a-3c for the low- and medium-mass scenarios. The background model fits the data well within the uncertainty propagated from the templates (hatched area). According to the fit, the templates associated with production of three b jets provide the dominant contribution to the background.

Subsequently, a signal template is included together with the background templates in the fit, with its fraction f_{sig} also allowed to vary freely. The fit is performed for Higgs boson masses from 90 to 350 GeV. The fit for a Higgs boson mass of 200 GeV in the medium-mass scenario is illustrated in Fig. 3d.

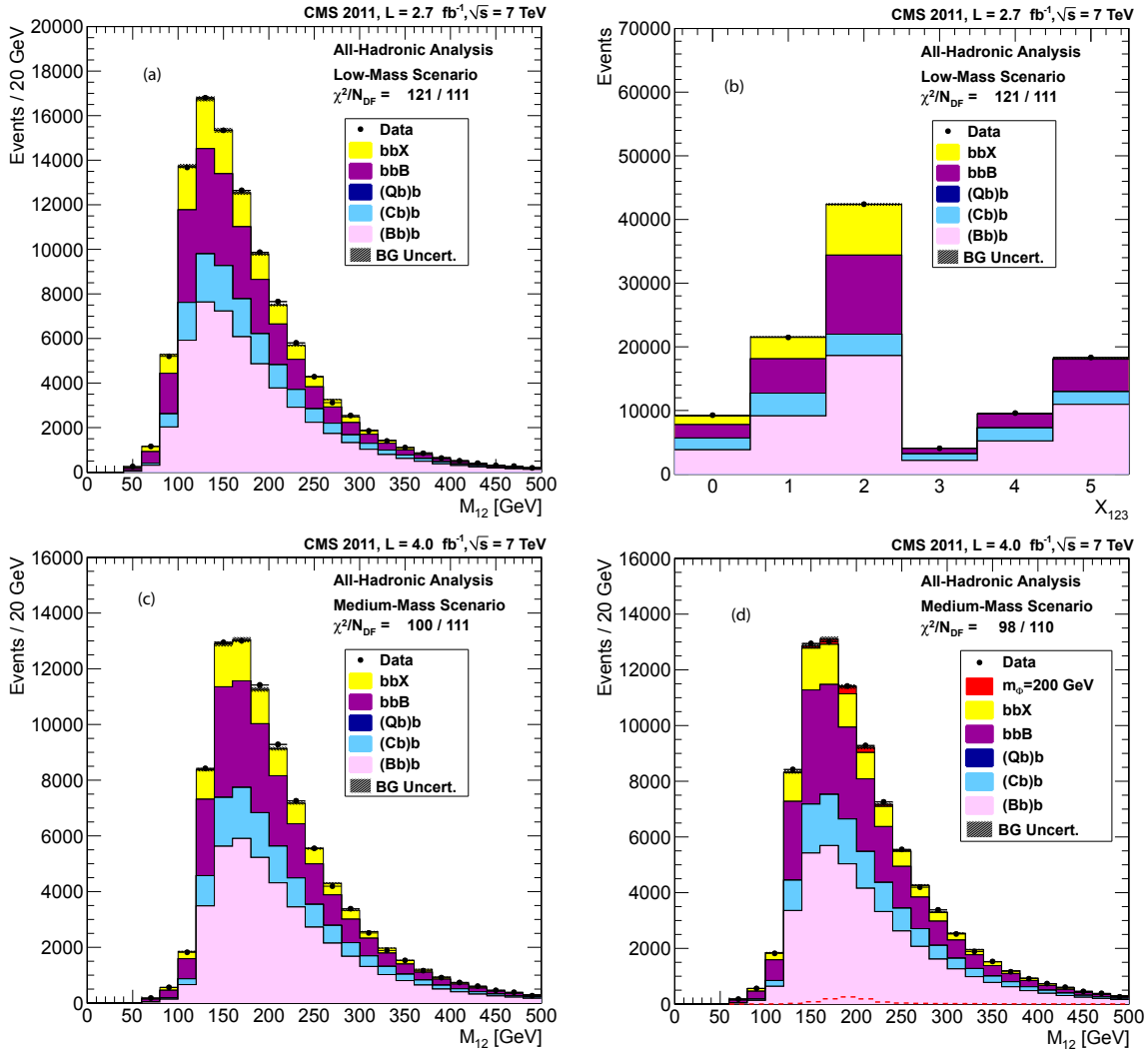


Figure 3: Results from the all-hadronic analysis. Top row: Result of the background-only fit in the triple-b-tag samples. The plot (a) shows the distribution of the dijet mass, M_{12} , the plot (b) the distribution of the event b-tag variable X_{123} in the low-mass scenario. The hatched area at the edge of the summed background histogram corresponds to the uncertainty propagated from the templates. Bottom row: Dijet mass distribution in the medium-mass scenario, (c) with the background-only fit, and (d) including an additional signal template for a MSSM Higgs boson with a mass of 200 GeV. The fitted mass distribution of the Higgs contribution is shown a second time as the dashed histogram at the bottom of the figure. The fitted contribution of the (Qb)b template is compatible with zero within errors.

The semileptonic analysis uses a binned likelihood fit to the invariant mass distribution of the two leading jets in the event to extract a possible MSSM Higgs contribution. Two different background predictions are considered, for the low- and medium-mass regions, which are fitted separately. In the fit the shape and normalisation of the background component are constrained through nuisance parameters as explained in section 6. The predicted background is shown in Fig. 4 for the two mass ranges, together with an expected signal for two Higgs boson

masses at $\tan\beta = 30$.

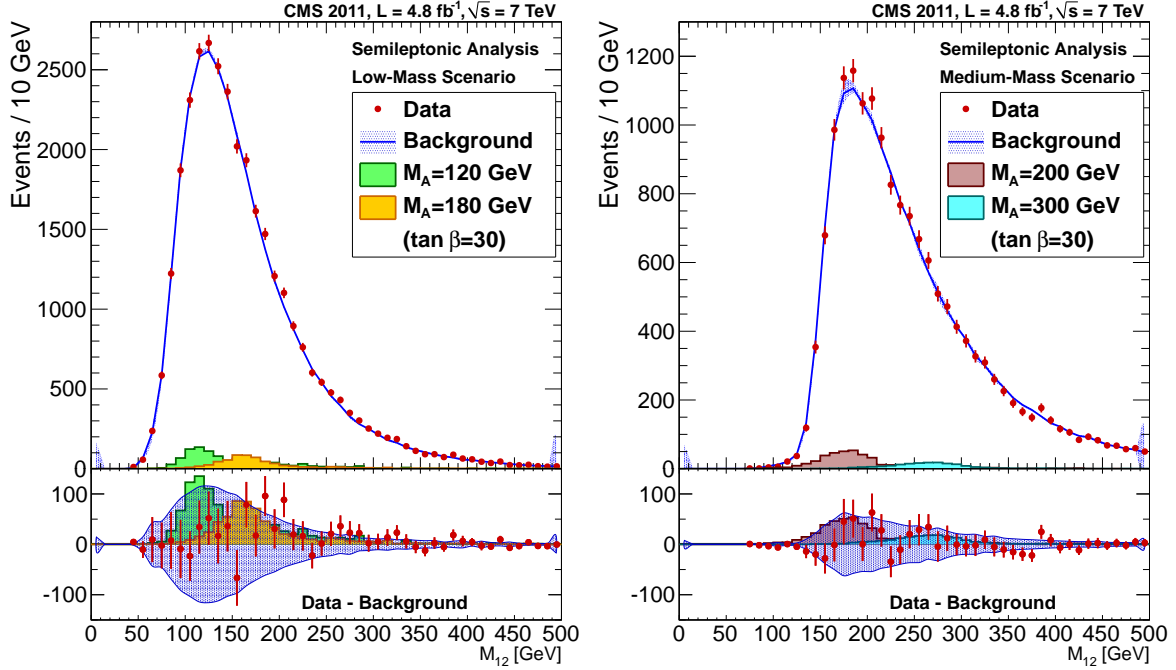


Figure 4: Results from the semileptonic analysis. Data (red) and predicted background (blue) in the signal region, for (left) low-mass range (used for $M_\phi \leq 180$ GeV) and (right) medium-mass range (used for $M_\phi > 180$ GeV); the expected signal for different M_A and for $\tan\beta = 30$ in the m_h^{\max} scenario, as described in the text, is also plotted. The difference between data and predicted background is also shown: the blue area represent the systematic and statistical uncertainties on the background prediction.

No significant deviation from background is observed in either analysis, and the CL_s [34–37] criterion is used to combine both results and determine the 95% confidence level (CL) limit on the signal contribution in the data, using the ROOSTATS [38] package. To avoid correlations, in the all-hadronic analysis the events common to the semileptonic case are removed from the triple-b-tag samples. The fractions of events removed in the all-hadronic data samples are 2.3% and 2.7% for the low- and medium-mass scenarios, respectively. The requirement of a muon in the semileptonic analysis and the harder kinematic selections of the all-hadronic analysis are responsible for such small overlap. Overlapping events in the simulated signal samples are also removed, although they are found to have negligible effect on the shape of the signal templates.

Results are shown graphically in Fig. 5 in terms of cross section times branching fraction, and reported in Table 2. There is generally good agreement between the observed and expected upper limits within statistical errors, and no indication of a signal is seen. The observed upper limits range from about 312 pb at $M_\phi = 90$ GeV to about 4 pb at $M_\phi = 350$ GeV. The individual observed limits of the two signatures are also displayed. The all-hadronic signature has a generally larger signal efficiency, but requires higher thresholds for jet energies, while the presence of a muon in the semileptonic signature allows for lower thresholds at the cost of lower signal efficiency. As a result, both signatures are comparable in sensitivity.

Figure 6 presents the results in the MSSM framework as a function of the MSSM parameters M_A and $\tan\beta$, combining the individual results of the two analyses, including all the statistical and systematic uncertainties as well as correlations. We use the MSSM m_h^{\max} benchmark sce-

nario [39, 40], which is designed to maximize the theoretical upper bound on M_h for a given $\tan\beta$ and fixed M_{SUSY} . Even though its parameters are under tension with the latest experimental results [41], it is currently still the most suitable benchmark scenario to compare the sensitivity of different analyses channels. The definition of theory parameters in the m_h^{max} benchmark scenario is the following: $M_{\text{SUSY}} = 1 \text{ TeV}$; $X_t = 2M_{\text{SUSY}}$; $\mu = 200 \text{ GeV}$; $M_{\tilde{g}} = 800 \text{ GeV}$; $M_2 = 200 \text{ GeV}$; and $A_b = A_t$; $M_3 = 800 \text{ GeV}$. Here, M_{SUSY} denotes the common soft-SUSY-breaking squark mass of the third generation; $X_t = A_t - \mu / \tan\beta^2$ is the stop mixing parameter; A_t and A_b are the stop and sbottom trilinear couplings, respectively; μ is the Higgsino mass parameter; $M_{\tilde{g}}$ is the gluino mass; and M_2 is the SU(2)-gaugino mass parameter. The value of M_1 is fixed via the unification relation $M_1 = (5/3)M_2 \sin\theta_W / \cos\theta_W$. The expected cross section and branching fraction, in the MSSM framework, are calculated by BBH@NNLO [42], in the 5-flavor scheme, and FEYNHIGGS [43–46], respectively. Exclusion plots for two values of $\mu = \pm 200 \text{ GeV}$ are shown.

Figure 7 shows the results in the scenario with $\mu = -200 \text{ GeV}$, together with previous limits set by Tevatron [12] in the multi-b jet final state, and by LEP [8]. In particular, no excess over the expected SM background is found for high values of $\tan\beta$ and for a resonance in the 100–150 GeV mass range, as previously reported by CDF and D0. The result of this work extends the sensitivity for MSSM searches in the $\phi \rightarrow b\bar{b}$ decay mode to much lower values of $\tan\beta$, excluding the region where the excess was reported.

The combined results reported in this Letter, using only the data collected at the LHC with a center-of-mass of $\sqrt{s} = 7 \text{ TeV}$, provides the most stringent limits on neutral Higgs boson decay in the $b\bar{b}$ mode, produced in association with b quarks.

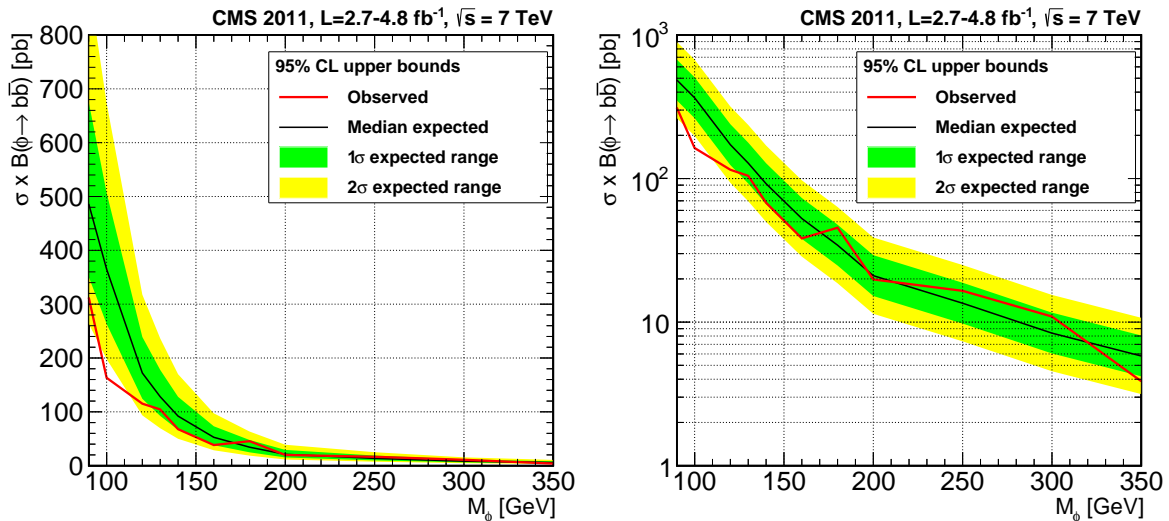


Figure 5: Observed and expected upper limits for the cross section times branching fraction at 95% CL, with linear (left) and logarithmic (right) scales, including statistical and systematic uncertainties for the combined all-hadronic and semileptonic results. One- and two-standard deviation ranges for the expected upper limit are also shown.

8 Summary and conclusions

We searched for a Higgs boson decaying into a pair of b quarks, produced in association with one or more additional b-quark jets. We used data samples corresponding to an integrated luminosity of $2.7\text{--}4.8 \text{ fb}^{-1}$ collected in 2011 in proton-proton collisions at a center-of-mass energy

Table 2: Expected and observed upper limits at 95% CL on $\sigma(\text{pp} \rightarrow \text{b}\phi + \text{X}) \times \mathcal{B}(\phi \rightarrow \text{b}\bar{\text{b}})$, in pb, and on $\tan\beta$ in the m_h^{max} benchmark scenario for two values of the parameter $\mu = \pm 200$ GeV.

$M_A(\text{GeV})$	$\sigma(\text{pp} \rightarrow \text{b}\phi + \text{X}) \times \mathcal{B}(\phi \rightarrow \text{b}\bar{\text{b}})$ [pb]		$\tan\beta$ ($\mu = +200$ GeV)		$\tan\beta$ ($\mu = -200$ GeV)	
	expected	observed	expected	observed	expected	observed
90	486.3	312.4	28.2	21.8	23.4	18.7
100	365.1	163.2	28.2	17.7	23.5	15.7
120	172.1	115.2	25.7	20.5	22.0	18.1
130	128.1	104.5	24.8	21.9	21.2	19.1
140	92.0	67.8	25.1	21.2	21.3	18.4
160	52.7	38.3	23.2	19.5	19.8	17.0
180	34.4	45.5	23.5	27.8	19.9	23.0
200	21.1	19.8	22.2	21.6	19.0	18.5
250	13.5	16.5	29.1	32.6	23.7	26.1
300	8.4	10.9	35.7	42.2	27.9	31.8
350	5.8	3.9	44.0	35.5	33.0	28.0

of 7 TeV at the LHC. The data were collected with dedicated multijet triggers including b-tag selection, utilizing both all-hadronic and semileptonic event signatures.

The search was performed on a triple-b-tag sample, using the invariant mass of two leading jets as a discriminating variable, with a prediction of the multijet background using control data samples. The all-hadronic analysis makes use of a second discriminating variable, X_{123} , that reflects the heavy flavor content of the event.

No signal is observed above the SM background expectations, and 95% confidence level upper limits on the $\text{pp} \rightarrow \text{b}\phi + \text{X}$, $\phi \rightarrow \text{b}\bar{\text{b}}$ cross section times branching fraction are derived in the 90–350 GeV mass range. These results are interpreted, in the MSSM model and the m_h^{max} scenario, in terms of bounds in the space of the parameters, M_A and $\tan\beta$. The 95% confidence level bound on $\tan\beta$ varies from about 18 to 42 in this Higgs boson mass range, thus excluding a region of parameter space previously unexplored for this final state.

Acknowledgements

We congratulate our colleagues in the CERN accelerator departments for the excellent performance of the LHC and thank the technical and administrative staffs at CERN and at other CMS institutes for their contributions to the success of the CMS effort. In addition, we gratefully acknowledge the computing centers and personnel of the Worldwide LHC Computing Grid for delivering so effectively the computing infrastructure essential to our analyses. Finally, we acknowledge the enduring support for the construction and operation of the LHC and the CMS detector provided by the following funding agencies: BMWF and FWF (Austria); FNRS and FWO (Belgium); CNPq, CAPES, FAPERJ, and FAPESP (Brazil); MEYS (Bulgaria); CERN; CAS, MoST, and NSFC (China); COLCIENCIAS (Colombia); MSES (Croatia); RPF (Cyprus); MoER, SF0690030s09 and ERDF (Estonia); Academy of Finland, MEC, and HIP (Finland); CEA and CNRS/IN2P3 (France); BMBF, DFG, and HGF (Germany); GSRT (Greece); OTKA and NKTH (Hungary); DAE and DST (India); IPM (Iran); SFI (Ireland); INFN (Italy); NRF and WCU (Republic of Korea); LAS (Lithuania); CINVESTAV, CONACYT, SEP, and UASLP-FAI (Mexico); MSI (New Zealand); PAEC (Pakistan); MSHE and NSC (Poland); FCT (Portugal); JINR (Armenia, Belarus, Georgia, Ukraine, Uzbekistan); MON, RosAtom, RAS and RFBR (Russia); MSTD

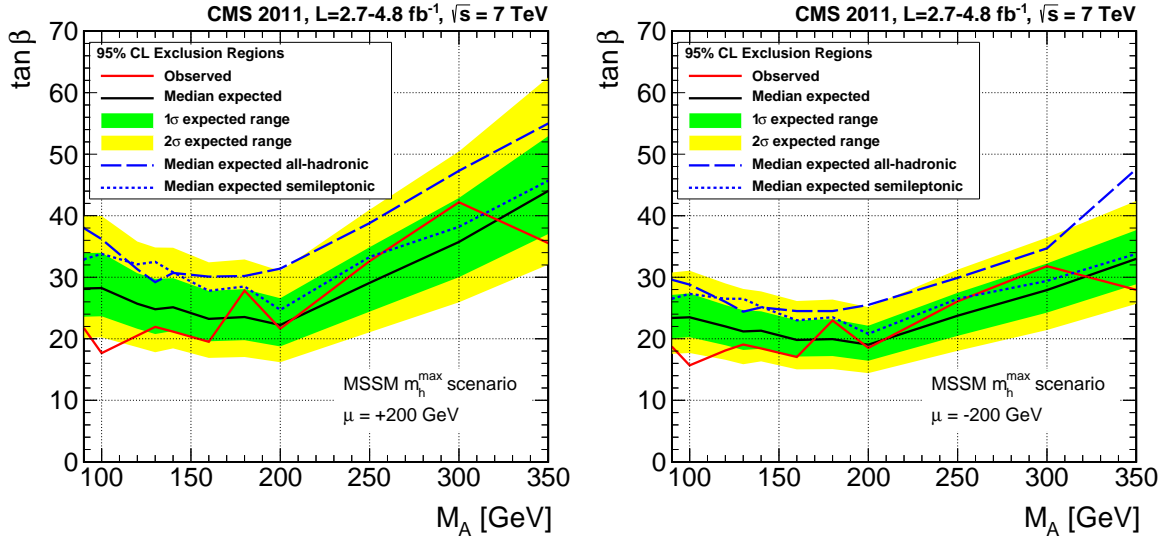


Figure 6: Observed upper limits at 95% CL on $\tan\beta$ as a function of M_A , including the statistical and systematic uncertainties, in the m_h^{\max} benchmark scenario, both for $\mu = +200$ GeV (left) and $\mu = -200$ GeV (right), for the combined all-hadronic and semileptonic results. One- and two-standard deviation ranges for the expected upper limit are represented by the color bands. The expected upper limits for each of two signatures are also shown (dashed and dotted lines).

(Serbia); SEIDI and CPAN (Spain); Swiss Funding Agencies (Switzerland); NSC (Taipei); ThEP-Center, IPST and NSTDA (Thailand); TUBITAK and TAEK (Turkey); NASU (Ukraine); STFC (United Kingdom); DOE and NSF (USA). Individuals have received support from the Marie-Curie programme and the European Research Council (European Union); the Leventis Foundation; the A. P. Sloan Foundation; the Alexander von Humboldt Foundation; the Belgian Federal Science Policy Office; the Fonds pour la Formation à la Recherche dans l'Industrie et dans l'Agriculture (FRIA-Belgium); the Agentschap voor Innovatie door Wetenschap en Technologie (IWT-Belgium); the Ministry of Education, Youth and Sports (MEYS) of Czech Republic; the Council of Science and Industrial Research, India; the Compagnia di San Paolo (Torino); and the HOMING PLUS programme of Foundation for Polish Science, cofinanced from European Union, Regional Development Fund.

References

- [1] ATLAS Collaboration, "Observation of a new particle in the search for the Standard Model Higgs boson with the ATLAS detector at the LHC", *Phys. Lett. B* **716** (2012) 1, doi:10.1016/j.physletb.2012.08.020, arXiv:1207.7214.
- [2] CMS Collaboration, "Observation of a new boson at a mass of 125 GeV with the CMS experiment at the LHC", *Phys. Lett. B* **716** (2012) 30, doi:10.1016/j.physletb.2012.08.021, arXiv:1207.7235.
- [3] E. Witten, "Mass Hierarchies in Supersymmetric Theories", *Phys. Lett. B* **105** (1981) 267, doi:10.1016/0370-2693(81)90885-6.
- [4] S. P. Martin, "A Supersymmetry Primer", (1997). arXiv:hep-ph/9709356. And references therein.

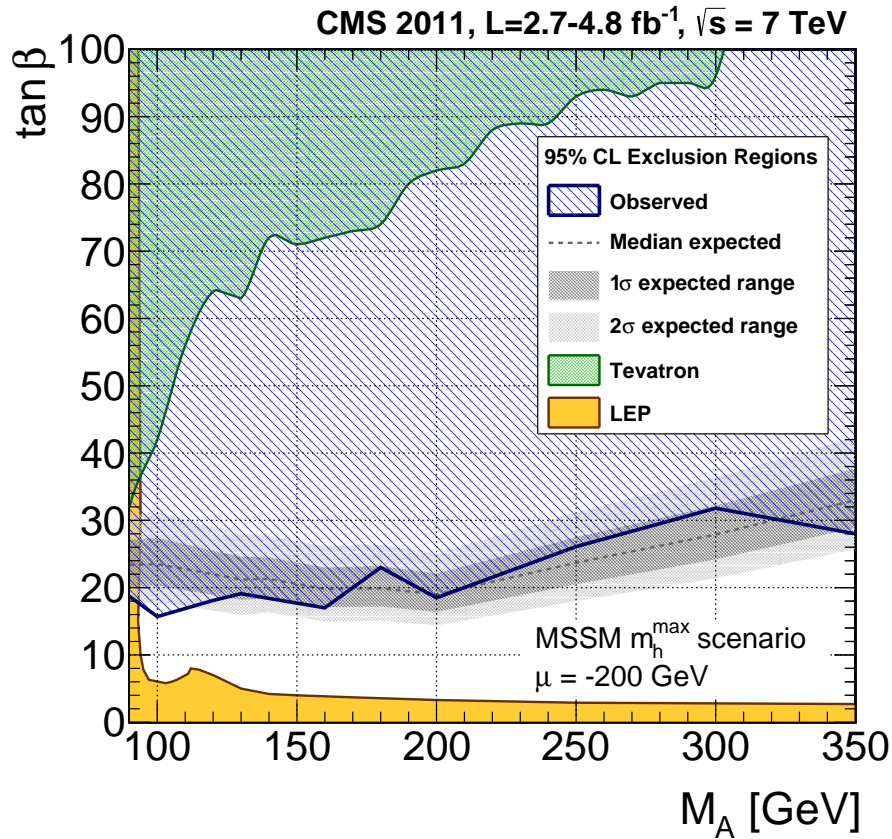


Figure 7: Observed upper limits at 95% CL on $\tan \beta$ as a function of M_A , including the statistical and systematic uncertainties, in the m_h^{\max} benchmark scenario with $\mu = -200$ GeV for the combined all-hadronic and semileptonic results. One- and two-standard deviation ranges for the expected upper limit are represented by the gray bands. Previous exclusion regions from LEP [8] and Tevatron in the multi-b jet channel [12] are overlaid.

- [5] H. P. Nilles, “Supersymmetry, supergravity and particle physics”, *Physics Reports* **110** (1984) 1, doi:10.1016/0370-1573(84)90008-5.
- [6] CMS Collaboration, “Search for neutral Higgs bosons decaying to tau pairs in pp collisions at $\sqrt{s} = 7$ TeV”, *Phys. Lett. B* **713** (2012) 68, doi:10.1016/j.physletb.2012.05.028, arXiv:1202.4083.
- [7] ATLAS Collaboration, “Search for the neutral Higgs bosons of the Minimal Supersymmetric Standard Model in pp collisions at $\sqrt{s} = 7$ TeV with the ATLAS detector”, (2012). arXiv:1211.6956. Submitted to JHEP.
- [8] ALEPH, DELPHI, L3, and OPAL Collaborations, LEP Working Group for Higgs Boson Searches, S. Schael, et al., “Search for neutral MSSM Higgs bosons at LEP”, *Eur. Phys. J. C* **47** (2006) 547, doi:10.1140/epjc/s2006-02569-7, arXiv:hep-ex/0602042.
- [9] CDF Collaboration, “Search for Higgs bosons predicted in two-Higgs-doublet models via decays to tau lepton pairs in 1.96-TeV $p\bar{p}$ collisions”, *Phys. Rev. Lett.* **103** (2009) 201801, doi:10.1103/PhysRevLett.103.201801, arXiv:0906.1014.

- [10] D0 Collaboration, “Search for Higgs bosons decaying to τ pairs in $p\bar{p}$ collisions with the D0 detector”, *Phys. Rev. Lett.* **101** (2008) 071804, doi:10.1103/PhysRevLett.101.071804, arXiv:0805.2491.
- [11] CMS Collaboration, “Search for Higgs bosons of the minimal supersymmetric standard model $p\bar{p}$ in collisions at $\sqrt{s} = 1.96$ TeV”, *Phys. Lett. B* **710** (2012) 569, doi:10.1016/j.physletb.2012.03.021, arXiv:1112.5431.
- [12] CDF and D0 Collaboration, “Search for neutral Higgs bosons in events with multiple bottom quarks at the Tevatron”, *Phys. Rev. D* **86** (2012) 091101, doi:10.1103/PhysRevD.86.091101, arXiv:1207.2757.
- [13] CMS Collaboration, “CMS technical design report, volume II: Physics performance”, *J. Phys. G* **34** (2007) 995, doi:10.1088/0954-3899/34/6/S01.
- [14] M. Carena et al., “LHC discovery potential for non-standard Higgs bosons in the $3b$ channel”, *JHEP* **07** (2012) 091, doi:10.1007/JHEP07(2012)091, arXiv:1203.1041.
- [15] CMS Collaboration, “The CMS experiment at the CERN LHC”, *JINST* **3** (2008) S08004, doi:10.1088/1748-0221/3/08/S08004.
- [16] CMS Collaboration, “Particle-flow event reconstruction in CMS and performance for jets, taus, and E_T^{miss} ”, CMS Physics Analysis Summary CMS-PAS-PFT-09-001, CERN, (2009).
- [17] CMS Collaboration, “Commissioning of the particle-flow event reconstruction with the first LHC collisions recorded in the CMS detector”, CMS Physics Analysis Summary CMS-PAS-PFT-10-001, CERN, (2010).
- [18] M. Cacciari, G. P. Salam, and G. Soyez, “The anti- k_t jet clustering algorithm”, *JHEP* **4** (2008) 63, doi:10.1088/1126-6708/2008/04/063, arXiv:0802.1189.
- [19] CMS Collaboration, “Determination of jet energy calibration and transverse momentum resolution in CMS”, *JINST* **6** (2011) P11002, doi:10.1088/1748-0221/6/11/P11002, arXiv:1107.4277.
- [20] CMS Collaboration, “Performance of CMS muon reconstruction in pp collision events at $\sqrt{s} = 7$ TeV”, *J. Instrum.* **7** (2012) P10002, doi:10.1088/1748-0221/7/10/P10002.
- [21] CMS Collaboration, “Identification of b-quark jets with the CMS experiment”, (2012). arXiv:1211.4462. Submitted to *JINST*.
- [22] W. Waltenberger, “Adaptive Vertex Reconstruction”, CMS Note 2008/33, CERN, (2008).
- [23] GEANT4 Collaboration, “GEANT4—a simulation toolkit”, *Nucl. Instrum. Meth. A* **506** (2003) 250, doi:10.1016/S0168-9002(03)01368-8.
- [24] T. Sjöstrand, S. Mrenna, and P. Z. Skands, “PYTHIA 6.4 physics and manual”, *JHEP* **05** (2006) 026, doi:10.1088/1126-6708/2006/05/026.
- [25] LHC Higgs Cross Section Working Group Collaboration, “Handbook of LHC Higgs Cross Sections: 2. Differential Distributions”, (CERN, Geneva, 2012). arXiv:1201.3084.

- [26] M. L. Mangano et al., “ALPGEN, a generator for hard multiparton processes in hadronic collisions”, *JHEP* **7** (2003) 1, doi:10.1088/1126-6708/2003/07/001, arXiv:hep-ph/0206293.
- [27] J. Alwall et al., “MadGraph 5: going beyond”, *JHEP* **06** (2011) 128, doi:10.1007/JHEP06(2011)128, arXiv:1106.0522.
- [28] J. Pumplin et al., “New generation of parton distributions with uncertainties from global QCD analysis”, *JHEP* **7** (2002) 12, doi:10.1088/1126-6708/2002/07/012, arXiv:hep-ph/0201195.
- [29] CDF Collaboration, “Search for Higgs Bosons Produced in Association with b -quarks”, *Phys. Rev. D* **85** (2012) 032005, doi:10.1103/PhysRevD.85.032005, arXiv:1106.4782.
- [30] CMS Collaboration, “ b -jet identification in the CMS experiment”, CMS Physics Analysis Summary CMS-PAS-BTV-11-004, CERN, (2012).
- [31] CMS Collaboration, “Performance of b -jet identification in CMS”, CMS Physics Analysis Summary CMS-PAS-BTV-11-001, CERN, (2011).
- [32] Particle Data Group, J. Beringer, et al., “Review of Particle Physics”, *Phys. Rev. D* **86** (2012) 010001, doi:10.1103/PhysRevD.86.010001.
- [33] M. Botje et al., “The PDF4LHC Working Group Interim Recommendations”, (2011). arXiv:1101.0538.
- [34] G. Cowan et al., “Asymptotic formulae for likelihood-based tests of new physics”, *Eur. Phys. J. C* **71** (2011) 1554, doi:10.1140/epjc/s10052-011-1554-0, arXiv:1007.1727.
- [35] A. L. Read, “Presentation of search results: the CLs technique”, *J. Phys. G* **28** (2002) 2693, doi:10.1088/0954-3899/28/10/313.
- [36] T. Junk, “Confidence level computation for combining searches with small statistics”, *Nucl. Instrum. Meth. A* **434** (1999) 435, doi:10.1016/S0168-9002(99)00498-2, arXiv:hep-ex/9902006.
- [37] ATLAS and CMS Collaborations and LHC Higgs Combination Group, “Procedure for the LHC Higgs boson search combination in Summer 2011”, Technical Report ATL-PHYS-PUB-2011-11, CMS-NOTE-2011-005, CERN, (2011).
- [38] L. Moneta et al., “The RooStats Project”, in *13th International Workshop on Advanced Computing and Analysis Techniques in Physics Research (ACAT2010)*. PoS ACAT:057 (2010). arXiv:1009.1003. PoS ACAT:057 (2010).
- [39] M. Carena et al., “Suggestions for benchmark scenarios for MSSM Higgs boson searches at hadron colliders”, *Eur. Phys. J. C* **26** (2003) 601, doi:10.1140/epjc/s2002-01084-3, arXiv:hep-ph/0202167.
- [40] M. Carena et al., “MSSM Higgs boson searches at the Tevatron and the LHC: Impact of different benchmark scenarios”, *Eur. Phys. J. C* **45** (2006) 797, doi:10.1140/epjc/s2005-02470-y, arXiv:hep-ph/0511023.

- [41] M. Carena et al., “MSSM Higgs Boson Searches at the LHC: Benchmark Scenarios after the Discovery of a Higgs-like Particle”, [arXiv:hep-ph/1302.7033](https://arxiv.org/abs/hep-ph/1302.7033).
- [42] R. V. Harlander and W. B. Kilgore, “Higgs boson production in bottom quark fusion at next-to-next-to-leading order”, *Phys. Rev. D* **68** (2003) 013001, [doi:10.1103/PhysRevD.68.013001](https://doi.org/10.1103/PhysRevD.68.013001), [arXiv:hep-ph/0304035](https://arxiv.org/abs/hep-ph/0304035).
- [43] S. Heinemeyer, W. Hollik, and G. Weiglein, “FeynHiggs: A program for the calculation of the masses of the neutral CP even Higgs bosons in the MSSM”, *Comput. Phys. Commun.* **124** (2000) 76, [doi:10.1016/S0010-4655\(99\)00364-1](https://doi.org/10.1016/S0010-4655(99)00364-1), [arXiv:hep-ph/9812320](https://arxiv.org/abs/hep-ph/9812320).
- [44] S. Heinemeyer, W. Hollik, and G. Weiglein, “The masses of the neutral CP-even Higgs bosons in the MSSM: Accurate analysis at the two loop level”, *Eur. Phys. J. C* **9** (1999) 343, [doi:10.1007/s100529900006](https://doi.org/10.1007/s100529900006), [arXiv:hep-ph/9812472](https://arxiv.org/abs/hep-ph/9812472).
- [45] G. Degrandi et al., “Towards high precision predictions for the MSSM Higgs sector”, *Eur. Phys. J. C* **28** (2003) 133, [doi:10.1140/epjc/s2003-01152-2](https://doi.org/10.1140/epjc/s2003-01152-2), [arXiv:hep-ph/0212020](https://arxiv.org/abs/hep-ph/0212020).
- [46] M. Frank et al., “The Higgs boson masses and mixings of the complex MSSM in the Feynman-diagrammatic approach”, *JHEP* **02** (2007) 47, [doi:10.1088/1126-6708/2007/02/047](https://doi.org/10.1088/1126-6708/2007/02/047), [arXiv:hep-ph/0611326](https://arxiv.org/abs/hep-ph/0611326).

A The CMS Collaboration

Yerevan Physics Institute, Yerevan, Armenia

S. Chatrchyan, V. Khachatryan, A.M. Sirunyan, A. Tumasyan

Institut für Hochenergiephysik der OeAW, Wien, Austria

W. Adam, E. Aguilo, T. Bergauer, M. Dragicevic, J. Erö, C. Fabjan¹, M. Friedl, R. Frühwirth¹, V.M. Ghete, N. Hörmann, J. Hrubec, M. Jeitler¹, W. Kiesenhofer, V. Knünz, M. Krammer¹, I. Krätschmer, D. Liko, I. Mikulec, M. Pernicka[†], D. Rabady², B. Rahbaran, C. Rohringer, H. Rohringer, R. Schöfbeck, J. Strauss, A. Taurok, W. Waltenberger, C.-E. Wulz¹

National Centre for Particle and High Energy Physics, Minsk, Belarus

V. Mossolov, N. Shumeiko, J. Suarez Gonzalez

Universiteit Antwerpen, Antwerpen, Belgium

S. Alderweireldt, M. Bansal, S. Bansal, T. Cornelis, E.A. De Wolf, X. Janssen, S. Luyckx, L. Mucibello, S. Ochesanu, B. Roland, R. Rougny, M. Selvaggi, H. Van Haeevermaet, P. Van Mechelen, N. Van Remortel, A. Van Spilbeeck

Vrije Universiteit Brussel, Brussel, Belgium

F. Blekman, S. Blyweert, J. D'Hondt, R. Gonzalez Suarez, A. Kalogeropoulos, M. Maes, A. Olbrechts, S. Tavernier, W. Van Doninck, P. Van Mulders, G.P. Van Onsem, I. Villella

Université Libre de Bruxelles, Bruxelles, Belgium

B. Clerbaux, G. De Lentdecker, V. Dero, A.P.R. Gay, T. Hreus, A. Léonard, P.E. Marage, A. Mohammadi, T. Reis, L. Thomas, C. Vander Velde, P. Vanlaer, J. Wang

Ghent University, Ghent, Belgium

V. Adler, K. Bernaert, A. Cimmino, S. Costantini, G. Garcia, M. Grunewald, B. Klein, J. Lellouch, A. Marinov, J. McCartin, A.A. Ocampo Rios, D. Ryckbosch, M. Sigamani, N. Strobbe, F. Thyssen, M. Tytgat, S. Walsh, E. Yazgan, N. Zaganidis

Université Catholique de Louvain, Louvain-la-Neuve, Belgium

S. Basegmez, G. Bruno, R. Castello, L. Ceard, C. Delaere, T. du Pree, D. Favart, L. Forthomme, A. Giammanco³, J. Hollar, V. Lemaitre, J. Liao, O. Militaru, C. Nuttens, D. Pagano, A. Pin, K. Piotrkowski, J.M. Vizan Garcia

Université de Mons, Mons, Belgium

N. Belyi, T. Caebergs, E. Daubie, G.H. Hammad

Centro Brasileiro de Pesquisas Fisicas, Rio de Janeiro, Brazil

G.A. Alves, M. Correa Martins Junior, T. Martins, M.E. Pol, M.H.G. Souza

Universidade do Estado do Rio de Janeiro, Rio de Janeiro, Brazil

W.L. Aldá Júnior, W. Carvalho, A. Custódio, E.M. Da Costa, D. De Jesus Damiao, C. De Oliveira Martins, S. Fonseca De Souza, H. Malbouisson, M. Malek, D. Matos Figueiredo, L. Mundim, H. Nogima, W.L. Prado Da Silva, A. Santoro, L. Soares Jorge, A. Sznajder, A. Vilela Pereira

Universidade Estadual Paulista ^a, Universidade Federal do ABC ^b, São Paulo, Brazil

T.S. Anjos^b, C.A. Bernardes^b, F.A. Dias^{a,4}, T.R. Fernandez Perez Tomei^a, E.M. Gregores^b, C. Lagana^a, F. Marinho^a, P.G. Mercadante^b, S.F. Novaes^a, Sandra S. Padula^a

Institute for Nuclear Research and Nuclear Energy, Sofia, Bulgaria

V. Genchev², P. Iaydjiev², S. Piperov, M. Rodozov, S. Stoykova, G. Sultanov, V. Tcholakov, R. Trayanov, M. Vutova

University of Sofia, Sofia, Bulgaria

A. Dimitrov, R. Hadjiiska, V. Kozhuharov, L. Litov, B. Pavlov, P. Petkov

Institute of High Energy Physics, Beijing, China

J.G. Bian, G.M. Chen, H.S. Chen, C.H. Jiang, D. Liang, S. Liang, X. Meng, J. Tao, J. Wang, X. Wang, Z. Wang, H. Xiao, M. Xu, J. Zang, Z. Zhang

State Key Laboratory of Nuclear Physics and Technology, Peking University, Beijing, China

C. Asawatrangkuldee, Y. Ban, Y. Guo, Q. Li, W. Li, S. Liu, Y. Mao, S.J. Qian, D. Wang, L. Zhang, W. Zou

Universidad de Los Andes, Bogota, Colombia

C. Avila, C.A. Carrillo Montoya, J.P. Gomez, B. Gomez Moreno, A.F. Osorio Oliveros, J.C. Sanabria

Technical University of Split, Split, Croatia

N. Godinovic, D. Lelas, R. Plestina⁵, D. Polic, I. Puljak²

University of Split, Split, Croatia

Z. Antunovic, M. Kovac

Institute Rudjer Boskovic, Zagreb, Croatia

V. Brigljevic, S. Duric, K. Kadija, J. Luetic, D. Mekterovic, S. Morovic, L. Tikvica

University of Cyprus, Nicosia, Cyprus

A. Attikis, M. Galanti, G. Mavromanolakis, J. Mousa, C. Nicolaou, F. Ptochos, P.A. Razis

Charles University, Prague, Czech Republic

M. Finger, M. Finger Jr.

Academy of Scientific Research and Technology of the Arab Republic of Egypt, Egyptian Network of High Energy Physics, Cairo, Egypt

Y. Assran⁶, S. Elgammal⁷, A. Ellithi Kamel⁸, A.M. Kuotb Awad⁹, M.A. Mahmoud⁹, A. Radi^{10,11}

National Institute of Chemical Physics and Biophysics, Tallinn, Estonia

M. Kadastik, M. Müntel, M. Murumaa, M. Raidal, L. Rebane, A. Tiko

Department of Physics, University of Helsinki, Helsinki, Finland

P. Eerola, G. Fedi, M. Voutilainen

Helsinki Institute of Physics, Helsinki, Finland

J. Härkönen, A. Heikkinen, V. Karimäki, R. Kinnunen, M.J. Kortelainen, T. Lampén, K. Lassila-Perini, S. Lehti, T. Lindén, P. Luukka, T. Mäenpää, T. Peltola, E. Tuominen, J. Tuominiemi, E. Tuovinen, D. Ungaro, L. Wendland

Lappeenranta University of Technology, Lappeenranta, Finland

A. Korpela, T. Tuuva

DSM/IRFU, CEA/Saclay, Gif-sur-Yvette, France

M. Besancon, S. Choudhury, M. Dejardin, D. Denegri, B. Fabbro, J.L. Faure, F. Ferri, S. Ganjour, A. Givernaud, P. Gras, G. Hamel de Monchenault, P. Jarry, E. Locci, J. Malcles, L. Millischer, A. Nayak, J. Rander, A. Rosowsky, M. Titov

Laboratoire Leprince-Ringuet, Ecole Polytechnique, IN2P3-CNRS, Palaiseau, France

S. Baffioni, F. Beaudette, L. Benhabib, L. Bianchini, M. Bluj¹², P. Busson, C. Charlot, N. Daci, T. Dahms, M. Dalchenko, L. Dobrzynski, A. Florent, R. Granier de Cassagnac, M. Haguenaer,

P. Miné, C. Mironov, I.N. Naranjo, M. Nguyen, C. Ochando, P. Paganini, D. Sabes, R. Salerno, Y. Sirois, C. Veelken, A. Zabi

Institut Pluridisciplinaire Hubert Curien, Université de Strasbourg, Université de Haute Alsace Mulhouse, CNRS/IN2P3, Strasbourg, France

J.-L. Agram¹³, J. Andrea, D. Bloch, D. Bodin, J.-M. Brom, M. Cardaci, E.C. Chabert, C. Collard, E. Conte¹³, F. Drouhin¹³, J.-C. Fontaine¹³, D. Gelé, U. Goerlach, P. Juillot, A.-C. Le Bihan, P. Van Hove

Université de Lyon, Université Claude Bernard Lyon 1, CNRS-IN2P3, Institut de Physique Nucléaire de Lyon, Villeurbanne, France

S. Beauceron, N. Beaupere, O. Bondu, G. Boudoul, S. Brochet, J. Chasserat, R. Chierici², D. Contardo, P. Depasse, H. El Mamouni, J. Fay, S. Gascon, M. Gouzevitch, B. Ille, T. Kurca, M. Lethuillier, L. Mirabito, S. Perries, L. Sgandurra, V. Sordini, Y. Tschudi, P. Verdier, S. Viret

Institute of High Energy Physics and Informatization, Tbilisi State University, Tbilisi, Georgia

Z. Tsamalaidze¹⁴

RWTH Aachen University, I. Physikalisches Institut, Aachen, Germany

C. Autermann, S. Beranek, B. Calpas, M. Edelhoff, L. Feld, N. Heracleous, O. Hindrichs, R. Jussen, K. Klein, J. Merz, A. Ostapchuk, A. Perieanu, F. Raupach, J. Sammet, S. Schael, D. Sprenger, H. Weber, B. Wittmer, V. Zhukov¹⁵

RWTH Aachen University, III. Physikalisches Institut A, Aachen, Germany

M. Ata, J. Caudron, E. Dietz-Laursonn, D. Duchardt, M. Erdmann, R. Fischer, A. Güth, T. Hebbeker, C. Heidemann, K. Hoepfner, D. Klingebiel, P. Kreuzer, M. Merschmeyer, A. Meyer, M. Olschewski, K. Padeken, P. Papacz, H. Pieta, H. Reithler, S.A. Schmitz, L. Sonnenschein, J. Stegmann, D. Teyssier, S. Thüer, M. Weber

RWTH Aachen University, III. Physikalisches Institut B, Aachen, Germany

M. Bontenackels, V. Cherepanov, Y. Erdogan, G. Flügge, H. Geenen, M. Geisler, W. Haj Ahmad, F. Hoehle, B. Kargoll, T. Kress, Y. Kuessel, J. Lingemann², A. Nowack, I.M. Nugent, L. Perchalla, O. Pooth, P. Sauerland, A. Stahl

Deutsches Elektronen-Synchrotron, Hamburg, Germany

M. Aldaya Martin, I. Asin, J. Behr, W. Behrenhoff, U. Behrens, M. Bergholz¹⁶, A. Bethani, K. Borrás, A. Burgmeier, A. Cakir, L. Calligaris, A. Campbell, E. Castro, F. Costanza, D. Dammann, C. Diez Pardos, T. Dorland, G. Eckerlin, D. Eckstein, G. Flucke, A. Geiser, I. Glushkov, P. Gunnellini, S. Habib, J. Hauk, G. Hellwig, H. Jung, M. Kasemann, P. Katsas, C. Kleinwort, H. Kluge, A. Knutsson, M. Krämer, D. Krücker, E. Kuznetsova, W. Lange, J. Leonard, W. Lohmann¹⁶, B. Lutz, R. Mankel, I. Marfin, M. Marienfeld, I.-A. Melzer-Pellmann, A.B. Meyer, J. Mnich, A. Mussgiller, S. Naumann-Emme, O. Novgorodova, F. Nowak, J. Olzem, H. Perrey, A. Petrukhin, D. Pitzl, A. Raspereza, P.M. Ribeiro Cipriano, C. Riedl, E. Ron, M. Rosin, J. Salfeld-Nebgen, R. Schmidt¹⁶, T. Schoerner-Sadenius, N. Sen, A. Spiridonov, M. Stein, R. Walsh, C. Wissing

University of Hamburg, Hamburg, Germany

V. Blobel, H. Enderle, J. Erfle, U. Gebbert, M. Görner, M. Gosselink, J. Haller, T. Hermanns, R.S. Höing, K. Kaschube, G. Kaussen, H. Kirschenmann, R. Klanner, J. Lange, T. Peiffer, N. Pietsch, D. Rathjens, C. Sander, H. Schettler, P. Schleper, E. Schlieckau, A. Schmidt, M. Schröder, T. Schum, M. Seidel, J. Sibille¹⁷, V. Sola, H. Stadie, G. Steinbrück, J. Thomsen, L. Vanelderen

Institut für Experimentelle Kernphysik, Karlsruhe, Germany

C. Barth, J. Berger, C. Böser, T. Chwalek, W. De Boer, A. Descroix, A. Dierlamm, M. Feindt, M. Guthoff², C. Hackstein, F. Hartmann², T. Hauth², M. Heinrich, H. Held, K.H. Hoffmann, U. Husemann, I. Katkov¹⁵, J.R. Komaragiri, P. Lobelle Pardo, D. Martschei, S. Mueller, Th. Müller, M. Niegel, A. Nürnberg, O. Oberst, A. Oehler, J. Ott, G. Quast, K. Rabbertz, F. Ratnikov, N. Ratnikova, S. Röcker, F.-P. Schilling, G. Schott, H.J. Simonis, F.M. Stober, D. Troendle, R. Ulrich, J. Wagner-Kuhr, S. Wayand, T. Weiler, M. Zeise

Institute of Nuclear Physics "Demokritos", Aghia Paraskevi, Greece

G. Anagnostou, G. Daskalakis, T. Gerasis, S. Kesisoglou, A. Kyriakis, D. Loukas, I. Manolakos, A. Markou, C. Markou, E. Ntomari

University of Athens, Athens, Greece

L. Gouskos, T.J. Mertzimekis, A. Panagiotou, N. Saoulidou

University of Ioánnina, Ioánnina, Greece

I. Evangelou, C. Foudas, P. Kokkas, N. Manthos, I. Papadopoulos

KFKI Research Institute for Particle and Nuclear Physics, Budapest, Hungary

G. Bencze, C. Hajdu, P. Hidas, D. Horvath¹⁸, F. Sikler, V. Veszpremi, G. Vesztergombi¹⁹, A.J. Zsigmond

Institute of Nuclear Research ATOMKI, Debrecen, Hungary

N. Beni, S. Czellar, J. Molnar, J. Palinkas, Z. Szillasi

University of Debrecen, Debrecen, Hungary

J. Karancsi, P. Raics, Z.L. Trocsanyi, B. Ujvari

Panjab University, Chandigarh, India

S.B. Beri, V. Bhatnagar, N. Dhingra, R. Gupta, M. Kaur, M.Z. Mehta, M. Mittal, N. Nishu, L.K. Saini, A. Sharma, J.B. Singh

University of Delhi, Delhi, India

Ashok Kumar, Arun Kumar, S. Ahuja, A. Bhardwaj, B.C. Choudhary, S. Malhotra, M. Naimuddin, K. Ranjan, P. Saxena, V. Sharma, R.K. Shivpuri

Saha Institute of Nuclear Physics, Kolkata, India

S. Banerjee, S. Bhattacharya, K. Chatterjee, S. Dutta, B. Gomber, Sa. Jain, Sh. Jain, R. Khurana, A. Modak, S. Mukherjee, D. Roy, S. Sarkar, M. Sharan

Bhabha Atomic Research Centre, Mumbai, India

A. Abdulsalam, D. Dutta, S. Kailas, V. Kumar, A.K. Mohanty², L.M. Pant, P. Shukla

Tata Institute of Fundamental Research - EHEP, Mumbai, India

T. Aziz, R.M. Chatterjee, S. Ganguly, M. Guchait²⁰, A. Gurtu²¹, M. Maity²², G. Majumder, K. Mazumdar, G.B. Mohanty, B. Parida, K. Sudhakar, N. Wickramage

Tata Institute of Fundamental Research - HECR, Mumbai, India

S. Banerjee, S. Dugad

Institute for Research in Fundamental Sciences (IPM), Tehran, Iran

H. Arfaei²³, H. Bakhshiansohi, S.M. Etesami²⁴, A. Fahim²³, M. Hashemi²⁵, H. Hesari, A. Jafari, M. Khakzad, M. Mohammadi Najafabadi, S. Paktinat Mehdiabadi, B. Safarzadeh²⁶, M. Zeinali

INFN Sezione di Bari ^a, Università di Bari ^b, Politecnico di Bari ^c, Bari, Italy

M. Abbrescia^{a,b}, L. Barbone^{a,b}, C. Calabria^{a,b,2}, S.S. Chhibra^{a,b}, A. Colaleo^a, D. Creanza^{a,c}, N. De

Filippis^{a,c,2}, M. De Palma^{a,b}, L. Fiore^a, G. Iaselli^{a,c}, G. Maggi^{a,c}, M. Maggi^a, B. Marangelli^{a,b}, S. My^{a,c}, S. Nuzzo^{a,b}, N. Pacifico^a, A. Pompili^{a,b}, G. Pugliese^{a,c}, G. Selvaggi^{a,b}, L. Silvestris^a, G. Singh^{a,b}, R. Venditti^{a,b}, P. Verwilligen^a, G. Zito^a

INFN Sezione di Bologna ^a, Università di Bologna ^b, Bologna, Italy

G. Abbiendi^a, A.C. Benvenuti^a, D. Bonacorsi^{a,b}, S. Braibant-Giacomelli^{a,b}, L. Brigliadori^{a,b}, P. Capiluppi^{a,b}, A. Castro^{a,b}, F.R. Cavallo^a, M. Cuffiani^{a,b}, G.M. Dallavalle^a, F. Fabbri^a, A. Fanfani^{a,b}, D. Fasanella^{a,b}, P. Giacomelli^a, C. Grandi^a, L. Guiducci^{a,b}, S. Marcellini^a, G. Masetti^a, M. Meneghelli^{a,b,2}, A. Montanari^a, F.L. Navarria^{a,b}, F. Odorici^a, A. Perrotta^a, F. Primavera^{a,b}, A.M. Rossi^{a,b}, T. Rovelli^{a,b}, G.P. Siroli^{a,b}, N. Tosi, R. Travaglini^{a,b}

INFN Sezione di Catania ^a, Università di Catania ^b, Catania, Italy

S. Albergo^{a,b}, G. Cappello^{a,b}, M. Chiorboli^{a,b}, S. Costa^{a,b}, R. Potenza^{a,b}, A. Tricomi^{a,b}, C. Tuve^{a,b}

INFN Sezione di Firenze ^a, Università di Firenze ^b, Firenze, Italy

G. Barbagli^a, V. Ciulli^{a,b}, C. Civinini^a, R. D'Alessandro^{a,b}, E. Focardi^{a,b}, S. Frosali^{a,b}, E. Gallo^a, S. Gonzi^{a,b}, M. Meschini^a, S. Paoletti^a, G. Sguazzoni^a, A. Tropiano^{a,b}

INFN Laboratori Nazionali di Frascati, Frascati, Italy

L. Benussi, S. Bianco, S. Colafranceschi²⁷, F. Fabbri, D. Piccolo

INFN Sezione di Genova ^a, Università di Genova ^b, Genova, Italy

P. Fabbricatore^a, R. Musenich^a, S. Tosi^{a,b}

INFN Sezione di Milano-Bicocca ^a, Università di Milano-Bicocca ^b, Milano, Italy

A. Benaglia^a, F. De Guio^{a,b}, L. Di Matteo^{a,b,2}, S. Fiorendi^{a,b}, S. Gennai^{a,2}, A. Ghezzi^{a,b}, S. Malvezzi^a, R.A. Manzoni^{a,b}, A. Martelli^{a,b}, A. Massironi^{a,b}, D. Menasce^a, L. Moroni^a, M. Paganoni^{a,b}, D. Pedrini^a, S. Ragazzi^{a,b}, N. Redaelli^a, T. Tabarelli de Fatis^{a,b}

INFN Sezione di Napoli ^a, Università di Napoli 'Federico II' ^b, Università della Basilicata (Potenza) ^c, Università G. Marconi (Roma) ^d, Napoli, Italy

S. Buontempo^a, N. Cavallo^{a,c}, A. De Cosa^{a,b,2}, O. Dogangun^{a,b}, F. Fabozzi^{a,c}, A.O.M. Iorio^{a,b}, L. Lista^a, S. Meola^{a,d,28}, M. Merola^a, P. Paolucci^{a,2}

INFN Sezione di Padova ^a, Università di Padova ^b, Università di Trento (Trento) ^c, Padova, Italy

P. Azzi^a, N. Bacchetta^{a,2}, D. Bisello^{a,b}, A. Branca^{a,b,2}, R. Carlin^{a,b}, P. Checchia^a, T. Dorigo^a, F. Gasparini^{a,b}, U. Gasparini^{a,b}, A. Gozzelino^a, K. Kanishchev^{a,c}, S. Lacaprara^a, I. Lazzizzera^{a,c}, M. Margoni^{a,b}, A.T. Meneguzzo^{a,b}, J. Pazzini^{a,b}, N. Pozzobon^{a,b}, P. Ronchese^{a,b}, F. Simonetto^{a,b}, E. Torassa^a, M. Tosi^{a,b}, S. Vanini^{a,b}, P. Zotto^{a,b}, A. Zucchetta^{a,b}, G. Zumerle^{a,b}

INFN Sezione di Pavia ^a, Università di Pavia ^b, Pavia, Italy

M. Gabusi^{a,b}, S.P. Ratti^{a,b}, C. Riccardi^{a,b}, P. Torre^{a,b}, P. Vitulo^{a,b}

INFN Sezione di Perugia ^a, Università di Perugia ^b, Perugia, Italy

M. Biasini^{a,b}, G.M. Bilei^a, L. Fanò^{a,b}, P. Lariccia^{a,b}, G. Mantovani^{a,b}, M. Menichelli^a, A. Nappi^{a,b†}, F. Romeo^{a,b}, A. Saha^a, A. Santocchia^{a,b}, A. Spiezia^{a,b}, S. Taroni^{a,b}

INFN Sezione di Pisa ^a, Università di Pisa ^b, Scuola Normale Superiore di Pisa ^c, Pisa, Italy

P. Azzurri^{a,c}, G. Bagliesi^a, J. Bernardini^a, T. Boccali^a, G. Broccolo^{a,c}, R. Castaldi^a, R.T. D'Agnolo^{a,c,2}, R. Dell'Orso^a, F. Fiori^{a,b,2}, L. Foà^{a,c}, A. Giassi^a, A. Kraan^a, F. Ligabue^{a,c}, T. Lomtadze^a, L. Martini^{a,29}, A. Messineo^{a,b}, F. Palla^a, A. Rizzi^{a,b}, A.T. Serban^{a,30}, P. Spagnolo^a, P. Squillacioti^{a,2}, R. Tenchini^a, G. Tonelli^{a,b}, A. Venturi^a, P.G. Verdini^a

INFN Sezione di Roma ^a, Università di Roma ^b, Roma, Italy

L. Barone^{a,b}, F. Cavallari^a, D. Del Re^{a,b}, M. Diemoz^a, C. Fanelli^{a,b}, M. Grassi^{a,b,2}, E. Longo^{a,b}, P. Meridiani^{a,2}, F. Micheli^{a,b}, S. Nourbakhsh^{a,b}, G. Organtini^{a,b}, R. Paramatti^a, S. Rahatlou^{a,b}, L. Soffi^{a,b}

INFN Sezione di Torino ^a, Università di Torino ^b, Università del Piemonte Orientale (Novara) ^c, Torino, Italy

N. Amapane^{a,b}, R. Arcidiacono^{a,c}, S. Argiro^{a,b}, M. Arneodo^{a,c}, C. Biino^a, N. Cartiglia^a, S. Casasso^{a,b}, M. Costa^{a,b}, N. Demaria^a, C. Mariotti^{a,2}, S. Maselli^a, E. Migliore^{a,b}, V. Monaco^{a,b}, M. Musich^{a,2}, M.M. Obertino^{a,c}, G. Ortona^{a,b}, N. Pastrone^a, M. Pelliccioni^a, A. Potenza^{a,b}, A. Romero^{a,b}, R. Sacchi^{a,b}, A. Solano^{a,b}, A. Staiano^a

INFN Sezione di Trieste ^a, Università di Trieste ^b, Trieste, Italy

S. Belforte^a, V. Candolise^{a,b}, M. Casarsa^a, F. Cossutti^a, G. Della Ricca^{a,b}, B. Gobbo^a, M. Marone^{a,b,2}, D. Montanino^{a,b,2}, A. Penzo^a, A. Schizzi^{a,b}

Kangwon National University, Chunchon, Korea

T.Y. Kim, S.K. Nam

Kyungpook National University, Daegu, Korea

S. Chang, D.H. Kim, G.N. Kim, D.J. Kong, H. Park, D.C. Son, T. Son

Chonnam National University, Institute for Universe and Elementary Particles, Kwangju, Korea

J.Y. Kim, Zero J. Kim, S. Song

Korea University, Seoul, Korea

S. Choi, D. Gyun, B. Hong, M. Jo, H. Kim, T.J. Kim, K.S. Lee, D.H. Moon, S.K. Park, Y. Roh

University of Seoul, Seoul, Korea

M. Choi, J.H. Kim, C. Park, I.C. Park, S. Park, G. Ryu

Sungkyunkwan University, Suwon, Korea

Y. Choi, Y.K. Choi, J. Goh, M.S. Kim, E. Kwon, B. Lee, J. Lee, S. Lee, H. Seo, I. Yu

Vilnius University, Vilnius, Lithuania

M.J. Bilinskas, I. Grigelionis, M. Janulis, A. Juodagalvis

Centro de Investigacion y de Estudios Avanzados del IPN, Mexico City, Mexico

H. Castilla-Valdez, E. De La Cruz-Burelo, I. Heredia-de La Cruz, R. Lopez-Fernandez, J. Martínez-Ortega, A. Sanchez-Hernandez, L.M. Villasenor-Cendejas

Universidad Iberoamericana, Mexico City, Mexico

S. Carrillo Moreno, F. Vazquez Valencia

Benemerita Universidad Autonoma de Puebla, Puebla, Mexico

H.A. Salazar Ibarguen

Universidad Autónoma de San Luis Potosí, San Luis Potosí, Mexico

E. Casimiro Linares, A. Morelos Pineda, M.A. Reyes-Santos

University of Auckland, Auckland, New Zealand

D. Krofcheck

University of Canterbury, Christchurch, New Zealand

A.J. Bell, P.H. Butler, R. Doesburg, S. Reucroft, H. Silverwood

National Centre for Physics, Quaid-I-Azam University, Islamabad, Pakistan

M. Ahmad, M.I. Asghar, J. Butt, H.R. Hoorani, S. Khalid, W.A. Khan, T. Khurshid, S. Qazi, M.A. Shah, M. Shoaib

National Centre for Nuclear Research, Swierk, Poland

H. Bialkowska, B. Boimska, T. Frueboes, M. Górski, M. Kazana, K. Nawrocki, K. Romanowska-Rybinska, M. Szeleper, G. Wrochna, P. Zalewski

Institute of Experimental Physics, Faculty of Physics, University of Warsaw, Warsaw, Poland

G. Brona, K. Bunkowski, M. Cwiok, W. Dominik, K. Doroba, A. Kalinowski, M. Konecki, J. Krolikowski, M. Misiura

Laboratório de Instrumentação e Física Experimental de Partículas, Lisboa, Portugal

N. Almeida, P. Bargassa, A. David, P. Faccioli, P.G. Ferreira Parracho, M. Gallinaro, J. Seixas, J. Varela, P. Vischia

Joint Institute for Nuclear Research, Dubna, Russia

P. Bunin, I. Golutvin, I. Gorbunov, V. Karjavin, V. Konoplyanikov, G. Kozlov, A. Lanev, A. Malakhov, P. Moisezenz, V. Palichik, V. Perelygin, M. Savina, S. Shmatov, S. Shulha, V. Smirnov, A. Volodko, A. Zarubin

Petersburg Nuclear Physics Institute, Gatchina (St. Petersburg), Russia

S. Evstyukhin, V. Golovtsov, Y. Ivanov, V. Kim, P. Levchenko, V. Murzin, V. Oreshkin, I. Smirnov, V. Sulimov, L. Uvarov, S. Vavilov, A. Vorobyev, An. Vorobyev

Institute for Nuclear Research, Moscow, Russia

Yu. Andreev, A. Dermenev, S. Gninenko, N. Golubev, M. Kirsanov, N. Krasnikov, V. Matveev, A. Pashenkov, D. Tlisov, A. Toropin

Institute for Theoretical and Experimental Physics, Moscow, Russia

V. Epshteyn, M. Erofeeva, V. Gavrilov, M. Kossov, N. Lychkovskaya, V. Popov, G. Safronov, S. Semenov, I. Shreyber, V. Stolin, E. Vlasov, A. Zhokin

P.N. Lebedev Physical Institute, Moscow, Russia

V. Andreev, M. Azarkin, I. Dremin, M. Kirakosyan, A. Leonidov, G. Mesyats, S.V. Rusakov, A. Vinogradov

Skobeltsyn Institute of Nuclear Physics, Lomonosov Moscow State University, Moscow, Russia

A. Belyaev, E. Boos, V. Bunichev, M. Dubinin⁴, L. Dudko, A. Gribushin, V. Klyukhin, O. Kodolova, I. Lokhtin, A. Markina, S. Obraztsov, M. Perfilov, S. Petrushanko, A. Popov, L. Sarycheva[†], V. Savrin, A. Snigirev

State Research Center of Russian Federation, Institute for High Energy Physics, Protvino, Russia

I. Azhgirey, I. Bayshev, S. Bitioukov, V. Grishin², V. Kachanov, D. Konstantinov, V. Krychkin, V. Petrov, R. Ryutin, A. Sobol, L. Tourtchanovitch, S. Troshin, N. Tyurin, A. Uzunian, A. Volkov

University of Belgrade, Faculty of Physics and Vinca Institute of Nuclear Sciences, Belgrade, Serbia

P. Adzic³¹, M. Djordjevic, M. Ekmedzic, D. Krpic³¹, J. Milosevic

Centro de Investigaciones Energéticas Medioambientales y Tecnológicas (CIEMAT), Madrid, Spain

M. Aguilar-Benitez, J. Alcaraz Maestre, P. Arce, C. Battilana, E. Calvo, M. Cerrada, M. Chamizo

Llatas, N. Colino, B. De La Cruz, A. Delgado Peris, D. Domínguez Vázquez, C. Fernandez Bedoya, J.P. Fernández Ramos, A. Ferrando, J. Flix, M.C. Fouz, P. Garcia-Abia, O. Gonzalez Lopez, S. Goy Lopez, J.M. Hernandez, M.I. Josa, G. Merino, J. Puerta Pelayo, A. Quintario Olmeda, I. Redondo, L. Romero, J. Santaolalla, M.S. Soares, C. Willmott

Universidad Autónoma de Madrid, Madrid, Spain

C. Albajar, G. Codispoti, J.F. de Trocóniz

Universidad de Oviedo, Oviedo, Spain

H. Brun, J. Cuevas, J. Fernandez Menendez, S. Folgueras, I. Gonzalez Caballero, L. Lloret Iglesias, J. Piedra Gomez

Instituto de Física de Cantabria (IFCA), CSIC-Universidad de Cantabria, Santander, Spain

J.A. Brochero Cifuentes, I.J. Cabrillo, A. Calderon, S.H. Chuang, J. Duarte Campderros, M. Felcini³², M. Fernandez, G. Gomez, J. Gonzalez Sanchez, A. Graziano, C. Jorda, A. Lopez Virto, J. Marco, R. Marco, C. Martinez Rivero, F. Matorras, F.J. Munoz Sanchez, T. Rodrigo, A.Y. Rodríguez-Marrero, A. Ruiz-Jimeno, L. Scodellaro, I. Vila, R. Vilar Cortabitarte

CERN, European Organization for Nuclear Research, Geneva, Switzerland

D. Abbaneo, E. Auffray, G. Auzinger, M. Bachtis, P. Baillon, A.H. Ball, D. Barney, J.F. Benitez, C. Bernet⁵, G. Bianchi, P. Bloch, A. Bocci, A. Bonato, C. Botta, H. Breuker, T. Camporesi, G. Cerminara, T. Christiansen, J.A. Coarasa Perez, D. D'Enterria, A. Dabrowski, A. De Roeck, S. Di Guida, M. Dobson, N. Dupont-Sagorin, A. Elliott-Peisert, B. Frisch, W. Funk, G. Georgiou, M. Giffels, D. Gigi, K. Gill, D. Giordano, M. Girone, M. Giunta, F. Glege, R. Gomez-Reino Garrido, P. Govoni, S. Gowdy, R. Guida, S. Gundacker, J. Hammer, M. Hansen, P. Harris, C. Hartl, J. Harvey, B. Hegner, A. Hinzmann, V. Innocente, P. Janot, K. Kaadze, E. Karavakis, K. Kousouris, P. Lecoq, Y.-J. Lee, P. Lenzi, C. Lourenço, N. Magini, T. Mäki, M. Malberti, L. Malgeri, M. Mannelli, L. Masetti, F. Meijers, S. Mersi, E. Meschi, R. Moser, M. Mulders, P. Musella, E. Nesvold, L. Orsini, E. Palencia Cortezon, E. Perez, L. Perrozzi, A. Petrilli, A. Pfeiffer, M. Pierini, M. Pimiä, D. Piparo, G. Polese, L. Quertenmont, A. Racz, W. Reece, J. Rodrigues Antunes, G. Rolandi³³, C. Rovelli³⁴, M. Rovere, H. Sakulin, F. Santanastasio, C. Schäfer, C. Schwick, I. Segoni, S. Sekmen, A. Sharma, P. Siegrist, P. Silva, M. Simon, P. Sphicas³⁵, D. Spiga, A. Tsirou, G.I. Veres¹⁹, J.R. Vlimant, H.K. Wöhri, S.D. Worm³⁶, W.D. Zeuner

Paul Scherrer Institut, Villigen, Switzerland

W. Bertl, K. Deiters, W. Erdmann, K. Gabathuler, R. Horisberger, Q. Ingram, H.C. Kaestli, S. König, D. Kotlinski, U. Langenegger, F. Meier, D. Renker, T. Rohe

Institute for Particle Physics, ETH Zurich, Zurich, Switzerland

F. Bachmair, L. Bäni, P. Bortignon, M.A. Buchmann, B. Casal, N. Chanon, A. Deisher, G. Dissertori, M. Dittmar, M. Donegà, M. Dünser, P. Eller, J. Eugster, K. Freudenreich, C. Grab, D. Hits, P. Lecomte, W. Lustermann, A.C. Marini, P. Martinez Ruiz del Arbol, N. Mohr, F. Moortgat, C. Nägeli³⁷, P. Nef, F. Nessi-Tedaldi, F. Pandolfi, L. Pape, F. Pauss, M. Peruzzi, F.J. Ronga, M. Rossini, L. Sala, A.K. Sanchez, A. Starodumov³⁸, B. Stieger, M. Takahashi, L. Tauscher[†], A. Thea, K. Theofilatos, D. Treille, C. Urscheler, R. Wallny, H.A. Weber, L. Wehrli

Universität Zürich, Zurich, Switzerland

C. AMSLER³⁹, V. Chiochia, S. De Visscher, C. Favaro, M. Ivova Rikova, B. Kilminster, B. Millan Mejias, P. Otiougova, P. Robmann, H. Snoek, S. Tuppiti, M. Verzetti

National Central University, Chung-Li, Taiwan

Y.H. Chang, K.H. Chen, C. Ferro, C.M. Kuo, S.W. Li, W. Lin, Y.J. Lu, A.P. Singh, R. Volpe, S.S. Yu

National Taiwan University (NTU), Taipei, Taiwan

P. Bartalini, P. Chang, Y.H. Chang, Y.W. Chang, Y. Chao, K.F. Chen, C. Dietz, U. Grundler, W.-S. Hou, Y. Hsiung, K.Y. Kao, Y.J. Lei, R.-S. Lu, D. Majumder, E. Petrakou, X. Shi, J.G. Shiu, Y.M. Tzeng, X. Wan, M. Wang

Chulalongkorn University, Bangkok, Thailand

B. Asavapibhop, E. Simili, N. Srimanobhas, N. Suwonjandee

Cukurova University, Adana, Turkey

A. Adiguzel, M.N. Bakirci⁴⁰, S. Cerci⁴¹, C. Dozen, I. Dumanoglu, E. Eskut, S. Girgis, G. Gokbulut, E. Gurpinar, I. Hos, E.E. Kangal, T. Karaman, G. Karapinar⁴², A. Kayis Topaksu, G. Onengut, K. Ozdemir, S. Ozturk⁴³, A. Polatoz, K. Sogut⁴⁴, D. Sunar Cerci⁴¹, B. Tali⁴¹, H. Topakli⁴⁰, L.N. Vergili, M. Vergili

Middle East Technical University, Physics Department, Ankara, Turkey

I.V. Akin, T. Aliev, B. Bilin, S. Bilmis, M. Deniz, H. Gamsizkan, A.M. Guler, K. Ocalan, A. Ozpineci, M. Serin, R. Sever, U.E. Surat, M. Yalvac, E. Yildirim, M. Zeyrek

Bogazici University, Istanbul, Turkey

E. Gülmez, B. Isildak⁴⁵, M. Kaya⁴⁶, O. Kaya⁴⁶, S. Ozkorucuklu⁴⁷, N. Sonmez⁴⁸

Istanbul Technical University, Istanbul, Turkey

H. Bahtiyar, E. Barlas, K. Cankocak, Y.O. Günaydin⁴⁹, F.I. Vardarli, M. Yücel

National Scientific Center, Kharkov Institute of Physics and Technology, Kharkov, Ukraine

L. Levchuk

University of Bristol, Bristol, United Kingdom

J.J. Brooke, E. Clement, D. Cussans, H. Flacher, R. Frazier, J. Goldstein, M. Grimes, G.P. Heath, H.F. Heath, L. Kreczko, S. Metson, D.M. Newbold³⁶, K. Nirunpong, A. Poll, S. Senkin, V.J. Smith, T. Williams

Rutherford Appleton Laboratory, Didcot, United Kingdom

L. Basso⁵⁰, K.W. Bell, A. Belyaev⁵⁰, C. Brew, R.M. Brown, D.J.A. Cockerill, J.A. Coughlan, K. Harder, S. Harper, J. Jackson, B.W. Kennedy, E. Olaiya, D. Petyt, B.C. Radburn-Smith, C.H. Shepherd-Themistocleous, I.R. Tomalin, W.J. Womersley

Imperial College, London, United Kingdom

R. Bainbridge, G. Ball, R. Beuselinck, O. Buchmuller, D. Colling, N. Cripps, M. Cutajar, P. Dauncey, G. Davies, M. Della Negra, W. Ferguson, J. Fulcher, D. Futyan, A. Gilbert, A. Guneratne Bryer, G. Hall, Z. Hatherell, J. Hays, G. Iles, M. Jarvis, G. Karapostoli, L. Lyons, A.-M. Magnan, J. Marrouche, B. Mathias, R. Nandi, J. Nash, A. Nikitenko³⁸, J. Pela, M. Pesaresi, K. Petridis, M. Pioppi⁵¹, D.M. Raymond, S. Rogerson, A. Rose, C. Seez, P. Sharp[†], A. Sparrow, M. Stoye, A. Tapper, M. Vazquez Acosta, T. Virdee, S. Wakefield, N. Wardle, T. Whyntie

Brunel University, Uxbridge, United Kingdom

M. Chadwick, J.E. Cole, P.R. Hobson, A. Khan, P. Kyberd, D. Leggat, D. Leslie, W. Martin, I.D. Reid, P. Symonds, L. Teodorescu, M. Turner

Baylor University, Waco, USA

K. Hatakeyama, H. Liu, T. Scarborough

The University of Alabama, Tuscaloosa, USA

O. Charaf, C. Henderson, P. Rumerio

Boston University, Boston, USA

A. Avetisyan, T. Bose, C. Fantasia, A. Heister, P. Lawson, D. Lazic, J. Rohlf, D. Sperka, J. St. John, L. Sulak

Brown University, Providence, USA

J. Alimena, S. Bhattacharya, G. Christopher, D. Cutts, Z. Demiragli, A. Ferapontov, A. Garabedian, U. Heintz, S. Jabeen, G. Kukartsev, E. Laird, G. Landsberg, M. Luk, M. Narain, M. Segala, T. Sinthuprasith, T. Speer

University of California, Davis, Davis, USA

R. Breedon, G. Breto, M. Calderon De La Barca Sanchez, S. Chauhan, M. Chertok, J. Conway, R. Conway, P.T. Cox, J. Dolen, R. Erbacher, M. Gardner, R. Houtz, W. Ko, A. Kopecky, R. Lander, O. Mall, T. Miceli, D. Pellett, F. Ricci-Tam, B. Rutherford, M. Searle, J. Smith, M. Squires, M. Tripathi, R. Vasquez Sierra, R. Yohay

University of California, Los Angeles, USA

V. Andreev, D. Cline, R. Cousins, J. Duris, S. Erhan, P. Everaerts, C. Farrell, J. Hauser, M. Ignatenko, C. Jarvis, G. Rakness, P. Schlein[†], P. Traczyk, V. Valuev, M. Weber

University of California, Riverside, Riverside, USA

J. Babb, R. Clare, M.E. Dinardo, J. Ellison, J.W. Gary, F. Giordano, G. Hanson, H. Liu, O.R. Long, A. Luthra, H. Nguyen, S. Paramesvaran, J. Sturdy, S. Sumowidagdo, R. Wilken, S. Wimpenny

University of California, San Diego, La Jolla, USA

W. Andrews, J.G. Branson, G.B. Cerati, S. Cittolin, D. Evans, A. Holzner, R. Kelley, M. Lebourgeois, J. Letts, I. Macneill, B. Mangano, S. Padhi, C. Palmer, G. Petrucciani, M. Pieri, M. Sani, V. Sharma, S. Simon, E. Sudano, M. Tadel, Y. Tu, A. Vartak, S. Wasserbaech⁵², F. Würthwein, A. Yagil, J. Yoo

University of California, Santa Barbara, Santa Barbara, USA

D. Barge, R. Bellan, C. Campagnari, M. D'Alfonso, T. Danielson, K. Flowers, P. Geffert, C. George, F. Golf, J. Incandela, C. Justus, P. Kalavase, D. Kovalskyi, V. Krutelyov, S. Lowette, R. Magaña Villalba, N. Mccoll, V. Pavlunin, J. Ribnik, J. Richman, R. Rossin, D. Stuart, W. To, C. West

California Institute of Technology, Pasadena, USA

A. Apresyan, A. Bornheim, J. Bunn, Y. Chen, E. Di Marco, J. Duarte, M. Gataullin, D. Kcira, Y. Ma, A. Mott, H.B. Newman, C. Rogan, M. Spiropulu, V. Timciuc, J. Veverka, R. Wilkinson, S. Xie, Y. Yang, R.Y. Zhu

Carnegie Mellon University, Pittsburgh, USA

V. Azzolini, A. Calamba, R. Carroll, T. Ferguson, Y. Iiyama, D.W. Jang, Y.F. Liu, M. Paulini, H. Vogel, I. Vorobiev

University of Colorado at Boulder, Boulder, USA

J.P. Cumalat, B.R. Drell, W.T. Ford, A. Gaz, E. Luiggi Lopez, J.G. Smith, K. Stenson, K.A. Ulmer, S.R. Wagner

Cornell University, Ithaca, USA

J. Alexander, A. Chatterjee, N. Eggert, L.K. Gibbons, B. Heltsley, W. Hopkins, A. Khukhunaishvili, B. Kreis, N. Mirman, G. Nicolas Kaufman, J.R. Patterson, A. Ryd, E. Salvati, W. Sun, W.D. Teo, J. Thom, J. Thompson, J. Tucker, J. Vaughan, Y. Weng, L. Winstrom, P. Wittich

Fairfield University, Fairfield, USA

D. Winn

Fermi National Accelerator Laboratory, Batavia, USA

S. Abdullin, M. Albrow, J. Anderson, G. Apollinari, L.A.T. Bauerdick, A. Beretvas, J. Berryhill, P.C. Bhat, K. Burkett, J.N. Butler, V. Chetluru, H.W.K. Cheung, F. Chlebana, S. Cihangir, V.D. Elvira, I. Fisk, J. Freeman, Y. Gao, D. Green, O. Gutsche, J. Hanlon, R.M. Harris, J. Hirschauer, B. Hooberman, S. Jindariani, M. Johnson, U. Joshi, B. Klima, S. Kunori, S. Kwan, C. Leonidopoulos⁵³, J. Linacre, D. Lincoln, R. Lipton, J. Lykken, K. Maeshima, J.M. Marraffino, V.I. Martinez Outschoorn, S. Maruyama, D. Mason, P. McBride, K. Mishra, S. Mrenna, Y. Musienko⁵⁴, C. Newman-Holmes, V. O'Dell, E. Sexton-Kennedy, S. Sharma, W.J. Spalding, L. Spiegel, L. Taylor, S. Tkaczyk, N.V. Tran, L. Uplegger, E.W. Vaandering, R. Vidal, J. Whitmore, W. Wu, F. Yang, J.C. Yun

University of Florida, Gainesville, USA

D. Acosta, P. Avery, D. Bourilkov, M. Chen, T. Cheng, S. Das, M. De Gruttola, G.P. Di Giovanni, D. Dobur, A. Drozdetskiy, R.D. Field, M. Fisher, Y. Fu, I.K. Furic, J. Gartner, J. Hugon, B. Kim, J. Konigsberg, A. Korytov, A. Kropivnitskaya, T. Kypreos, J.F. Low, K. Matchev, P. Milenovic⁵⁵, G. Mitselmakher, L. Muniz, M. Park, R. Remington, A. Rinkevicius, P. Sellers, N. Skhirtladze, M. Snowball, J. Yelton, M. Zakaria

Florida International University, Miami, USA

V. Gaultney, S. Hewamanage, L.M. Lebolo, S. Linn, P. Markowitz, G. Martinez, J.L. Rodriguez

Florida State University, Tallahassee, USA

T. Adams, A. Askew, J. Bochenek, J. Chen, B. Diamond, S.V. Gleyzer, J. Haas, S. Hagopian, V. Hagopian, M. Jenkins, K.F. Johnson, H. Prosper, V. Veeraraghavan, M. Weinberg

Florida Institute of Technology, Melbourne, USA

M.M. Baarmand, B. Dorney, M. Hohlmann, H. Kalakhety, I. Vodopiyanov, F. Yumiceva

University of Illinois at Chicago (UIC), Chicago, USA

M.R. Adams, I.M. Anghel, L. Apanasevich, Y. Bai, V.E. Bazterra, R.R. Betts, I. Bucinskaite, J. Callner, R. Cavanaugh, O. Evdokimov, L. Gauthier, C.E. Gerber, D.J. Hofman, S. Khalatyan, F. Lacroix, C. O'Brien, C. Silkworth, D. Strom, P. Turner, N. Varelas

The University of Iowa, Iowa City, USA

U. Akgun, E.A. Albayrak, B. Bilki⁵⁶, W. Clarida, F. Duru, S. Griffiths, J.-P. Merlo, H. Mermerkaya⁵⁷, A. Mestvirishvili, A. Moeller, J. Nachtman, C.R. Newsom, E. Norbeck, Y. Onel, F. Ozok⁵⁸, S. Sen, P. Tan, E. Tiras, J. Wetzel, T. Yetkin, K. Yi

Johns Hopkins University, Baltimore, USA

B.A. Barnett, B. Blumenfeld, S. Bolognesi, D. Fehling, G. Giurgiu, A.V. Gritsan, Z.J. Guo, G. Hu, P. Maksimovic, M. Swartz, A. Whitbeck

The University of Kansas, Lawrence, USA

P. Baringer, A. Bean, G. Benelli, R.P. Kenny Iii, M. Murray, D. Noonan, S. Sanders, R. Stringer, G. Tinti, J.S. Wood

Kansas State University, Manhattan, USA

A.F. Barfuss, T. Bolton, I. Chakaberia, A. Ivanov, S. Khalil, M. Makouski, Y. Maravin, S. Shrestha, I. Svintradze

Lawrence Livermore National Laboratory, Livermore, USA

J. Gronberg, D. Lange, F. Rebassoo, D. Wright

University of Maryland, College Park, USA

A. Baden, B. Calvert, S.C. Eno, J.A. Gomez, N.J. Hadley, R.G. Kellogg, M. Kirn, T. Kolberg,

Y. Lu, M. Marionneau, A.C. Mignerey, K. Pedro, A. Peterman, A. Skuja, J. Temple, M.B. Tonjes, S.C. Tonwar

Massachusetts Institute of Technology, Cambridge, USA

A. Apyan, G. Bauer, J. Bendavid, W. Busza, E. Butz, I.A. Cali, M. Chan, V. Dutta, G. Gomez Ceballos, M. Goncharov, Y. Kim, M. Klute, K. Krajczar⁵⁹, A. Levin, P.D. Luckey, T. Ma, S. Nahn, C. Paus, D. Ralph, C. Roland, G. Roland, M. Rudolph, G.S.F. Stephans, F. Stöckli, K. Sumorok, K. Sung, D. Velicanu, E.A. Wenger, R. Wolf, B. Wyslouch, M. Yang, Y. Yilmaz, A.S. Yoon, M. Zanetti, V. Zhukova

University of Minnesota, Minneapolis, USA

S.I. Cooper, B. Dahmes, A. De Benedetti, G. Franzoni, A. Gude, S.C. Kao, K. Klapoetke, Y. Kubota, J. Mans, N. Pastika, R. Rusack, M. Sasseville, A. Singovsky, N. Tambe, J. Turkewitz

University of Mississippi, Oxford, USA

L.M. Cremaldi, R. Kroeger, L. Perera, R. Rahmat, D.A. Sanders

University of Nebraska-Lincoln, Lincoln, USA

E. Avdeeva, K. Bloom, S. Bose, D.R. Claes, A. Dominguez, M. Eads, J. Keller, I. Kravchenko, J. Lazo-Flores, S. Malik, G.R. Snow

State University of New York at Buffalo, Buffalo, USA

A. Godshalk, I. Iashvili, S. Jain, A. Kharchilava, A. Kumar, S. Rappoccio, Z. Wan

Northeastern University, Boston, USA

G. Alverson, E. Barberis, D. Baumgartel, M. Chasco, J. Haley, D. Nash, T. Orimoto, D. Trocino, D. Wood, J. Zhang

Northwestern University, Evanston, USA

A. Anastassov, K.A. Hahn, A. Kubik, L. Lusito, N. Mucia, N. Odell, R.A. Ofierzynski, B. Pollack, A. Pozdnyakov, M. Schmitt, S. Stoynev, M. Velasco, S. Won

University of Notre Dame, Notre Dame, USA

D. Berry, A. Brinkerhoff, K.M. Chan, M. Hildreth, C. Jessop, D.J. Karmgard, J. Kolb, K. Lannon, W. Luo, S. Lynch, N. Marinelli, D.M. Morse, T. Pearson, M. Planer, R. Ruchti, J. Slaunwhite, N. Valls, M. Wayne, M. Wolf

The Ohio State University, Columbus, USA

L. Antonelli, B. Bylsma, L.S. Durkin, C. Hill, R. Hughes, K. Kotov, T.Y. Ling, D. Puigh, M. Rodenburg, C. Vuosalo, G. Williams, B.L. Winer

Princeton University, Princeton, USA

E. Berry, P. Elmer, V. Halyo, P. Hebda, J. Hegeman, A. Hunt, P. Jindal, S.A. Koay, D. Lopes Pegna, P. Lujan, D. Marlow, T. Medvedeva, M. Mooney, J. Olsen, P. Piroué, X. Quan, A. Raval, H. Saka, D. Stickland, C. Tully, J.S. Werner, S.C. Zenz, A. Zuranski

University of Puerto Rico, Mayaguez, USA

E. Brownson, A. Lopez, H. Mendez, J.E. Ramirez Vargas

Purdue University, West Lafayette, USA

E. Alagoz, V.E. Barnes, D. Benedetti, G. Bolla, D. Bortoletto, M. De Mattia, A. Everett, Z. Hu, M. Jones, O. Koybasi, M. Kress, A.T. Laasanen, N. Leonardo, V. Maroussov, P. Merkel, D.H. Miller, N. Neumeister, I. Shipsey, D. Silvers, A. Svyatkovskiy, M. Vidal Marono, H.D. Yoo, J. Zablocki, Y. Zheng

Purdue University Calumet, Hammond, USA

S. Guragain, N. Parashar

Rice University, Houston, USA

A. Adair, B. Akgun, C. Boulahouache, K.M. Ecklund, F.J.M. Geurts, W. Li, B.P. Padley, R. Redjimi, J. Roberts, J. Zabel

University of Rochester, Rochester, USA

B. Betchart, A. Bodek, Y.S. Chung, R. Covarelli, P. de Barbaro, R. Demina, Y. Eshaq, T. Ferbel, A. Garcia-Bellido, P. Goldenzweig, J. Han, A. Harel, D.C. Miner, D. Vishnevskiy, M. Zielinski

The Rockefeller University, New York, USA

A. Bhatti, R. Ciesielski, L. Demortier, K. Goulios, G. Lungu, S. Malik, C. Mesropian

Rutgers, The State University of New Jersey, Piscataway, USA

S. Arora, A. Barker, J.P. Chou, C. Contreras-Campana, E. Contreras-Campana, D. Duggan, D. Ferencek, Y. Gershtein, R. Gray, E. Halkiadakis, D. Hidas, A. Lath, S. Panwalkar, M. Park, R. Patel, V. Rekovic, J. Robles, K. Rose, S. Salur, S. Schnetzer, C. Seitz, S. Somalwar, R. Stone, S. Thomas, M. Walker

University of Tennessee, Knoxville, USA

G. Cerizza, M. Hollingsworth, S. Spanier, Z.C. Yang, A. York

Texas A&M University, College Station, USA

R. Eusebi, W. Flanagan, J. Gilmore, T. Kamon⁶⁰, V. Khotilovich, R. Montalvo, I. Osipenkov, Y. Pakhotin, A. Perloff, J. Roe, A. Safonov, T. Sakuma, S. Sengupta, I. Suarez, A. Tatarinov, D. Toback

Texas Tech University, Lubbock, USA

N. Akchurin, J. Damgov, C. Dragoiu, P.R. Duderu, C. Jeong, K. Kovitanggoon, S.W. Lee, T. Libeiro, I. Volobouev

Vanderbilt University, Nashville, USA

E. Appelt, A.G. Delannoy, C. Florez, S. Greene, A. Gurrola, W. Johns, P. Kurt, C. Maguire, A. Melo, M. Sharma, P. Sheldon, B. Snook, S. Tuo, J. Velkovska

University of Virginia, Charlottesville, USA

M.W. Arenton, M. Balazs, S. Boutle, B. Cox, B. Francis, J. Goodell, R. Hirosky, A. Ledovskoy, C. Lin, C. Neu, J. Wood

Wayne State University, Detroit, USA

S. Gollapinni, R. Harr, P.E. Karchin, C. Kottachchi Kankanamge Don, P. Lamichhane, A. Sakharov

University of Wisconsin, Madison, USA

M. Anderson, D.A. Belknap, L. Borrello, D. Carlsmith, M. Cepeda, S. Dasu, E. Friis, L. Gray, K.S. Grogg, M. Grothe, R. Hall-Wilton, M. Herndon, A. Hervé, P. Klabbers, J. Klukas, A. Lanaro, C. Lazaridis, R. Loveless, A. Mohapatra, M.U. Mozer, I. Ojalvo, F. Palmonari, G.A. Pierro, I. Ross, A. Savin, W.H. Smith, J. Swanson

†: Deceased

1: Also at Vienna University of Technology, Vienna, Austria

2: Also at CERN, European Organization for Nuclear Research, Geneva, Switzerland

3: Also at National Institute of Chemical Physics and Biophysics, Tallinn, Estonia

4: Also at California Institute of Technology, Pasadena, USA

- 5: Also at Laboratoire Leprince-Ringuet, Ecole Polytechnique, IN2P3-CNRS, Palaiseau, France
- 6: Also at Suez Canal University, Suez, Egypt
- 7: Also at Zewail City of Science and Technology, Zewail, Egypt
- 8: Also at Cairo University, Cairo, Egypt
- 9: Also at Fayoum University, El-Fayoum, Egypt
- 10: Also at British University in Egypt, Cairo, Egypt
- 11: Now at Ain Shams University, Cairo, Egypt
- 12: Also at National Centre for Nuclear Research, Swierk, Poland
- 13: Also at Université de Haute Alsace, Mulhouse, France
- 14: Also at Joint Institute for Nuclear Research, Dubna, Russia
- 15: Also at Skobeltsyn Institute of Nuclear Physics, Lomonosov Moscow State University, Moscow, Russia
- 16: Also at Brandenburg University of Technology, Cottbus, Germany
- 17: Also at The University of Kansas, Lawrence, USA
- 18: Also at Institute of Nuclear Research ATOMKI, Debrecen, Hungary
- 19: Also at Eötvös Loránd University, Budapest, Hungary
- 20: Also at Tata Institute of Fundamental Research - HECR, Mumbai, India
- 21: Now at King Abdulaziz University, Jeddah, Saudi Arabia
- 22: Also at University of Visva-Bharati, Santiniketan, India
- 23: Also at Sharif University of Technology, Tehran, Iran
- 24: Also at Isfahan University of Technology, Isfahan, Iran
- 25: Also at Shiraz University, Shiraz, Iran
- 26: Also at Plasma Physics Research Center, Science and Research Branch, Islamic Azad University, Tehran, Iran
- 27: Also at Facoltà Ingegneria, Università di Roma, Roma, Italy
- 28: Also at Università degli Studi Guglielmo Marconi, Roma, Italy
- 29: Also at Università degli Studi di Siena, Siena, Italy
- 30: Also at University of Bucharest, Faculty of Physics, Bucuresti-Magurele, Romania
- 31: Also at Faculty of Physics, University of Belgrade, Belgrade, Serbia
- 32: Also at University of California, Los Angeles, USA
- 33: Also at Scuola Normale e Sezione dell'INFN, Pisa, Italy
- 34: Also at INFN Sezione di Roma, Roma, Italy
- 35: Also at University of Athens, Athens, Greece
- 36: Also at Rutherford Appleton Laboratory, Didcot, United Kingdom
- 37: Also at Paul Scherrer Institut, Villigen, Switzerland
- 38: Also at Institute for Theoretical and Experimental Physics, Moscow, Russia
- 39: Also at Albert Einstein Center for Fundamental Physics, Bern, Switzerland
- 40: Also at Gaziosmanpasa University, Tokat, Turkey
- 41: Also at Adiyaman University, Adiyaman, Turkey
- 42: Also at Izmir Institute of Technology, Izmir, Turkey
- 43: Also at The University of Iowa, Iowa City, USA
- 44: Also at Mersin University, Mersin, Turkey
- 45: Also at Ozyegin University, Istanbul, Turkey
- 46: Also at Kafkas University, Kars, Turkey
- 47: Also at Suleyman Demirel University, Isparta, Turkey
- 48: Also at Ege University, Izmir, Turkey
- 49: Also at Kahramanmaras Sütcü Imam University, Kahramanmaras, Turkey
- 50: Also at School of Physics and Astronomy, University of Southampton, Southampton, United Kingdom

51: Also at INFN Sezione di Perugia; Università di Perugia, Perugia, Italy

52: Also at Utah Valley University, Orem, USA

53: Now at University of Edinburgh, Scotland, Edinburgh, United Kingdom

54: Also at Institute for Nuclear Research, Moscow, Russia

55: Also at University of Belgrade, Faculty of Physics and Vinca Institute of Nuclear Sciences, Belgrade, Serbia

56: Also at Argonne National Laboratory, Argonne, USA

57: Also at Erzincan University, Erzincan, Turkey

58: Also at Mimar Sinan University, Istanbul, Istanbul, Turkey

59: Also at KFKI Research Institute for Particle and Nuclear Physics, Budapest, Hungary

60: Also at Kyungpook National University, Daegu, Korea